JPRS-UEE-91-001
29 JANUARY 1991

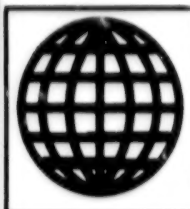

FOREIGN
BROADCAST
INFORMATION
SERVICE

JPRS Report

Science & Technology

USSR: Electronics & Electrical Engineering

Science & Technology

USSR: Electronics & Electrical Engineering

JPRS-UEE-91-001 29 January 1991

CONTENTS

Broadcasting, Consumer Electronics

Daylighting-90 International Conference [Unsigned; SVETOTEKHNIKA, No 10, Oct 90] 1
Analysis of Sky Brightness Distribution Models
[R. Kittler, L. Pirshel; SVETOTEKHNIKA, No 10, Oct 90] 1
The Brightness of the Urban Environment
[L. D. Bakharev, L. N. Orlova; SVETOTEKHNIKA, No 10, Oct 90] 1
Light-Transmitting Elements of Polymethyl Methacrylate and Polycarbonate
[U. Fisher; SVETOTEKHNIKA, No 10, Oct 90] 1
Engineering Method of Designing Natural Illumination Systems for Rooms With Effective Sun Protection [M. Yu. Mitnik, I. I. Spiridonov; SVETOTEKHNIKA, No 10, Oct 90] 1

Antennas, Propagation

Model of Variations in the Electronic Density Profiles of the Polar Ionospheric D-Layer as a Function of Riometric Absorption
[L. T. Zelenkova, T. A. Soldatov, et al.; GEOMAGNETIZM I AERONOMIYA, Vol 30 No 5, Sep-Oct 90] 2
Estimation of E-Layer Parameters From Long-Range Oblique Sounding Data
[R. Martin, L. Palasio, et al.; GEOMAGNETIZM I AERONOMIYA, Vol 30 No 5, Sep-Oct 90] 2
Propagation Features of Low-Frequency Electromagnetic Disturbances Caused by Ionospheric E-Layer Excitation [V. T. Surkov; GEOMAGNETIZM I AERONOMIYA, Vol 30 No 5, Sep-Oct 90] 2
Global Ionospheric Disturbances Generated by the Electrical Field From the "Morskaya Zvezda" Atomic Explosion on July 9, 1962
[Ye. Ye. Tsedilina; GEOMAGNETIZM I AERONOMIYA, Vol 30 No 5, Sep-Oct 90] 2
Global Ionospheric Perturbations Caused by the Electrical Field From the "Morskaya Zvezda" Atomic Explosion of July 9, 1962. Part II
[Ye. Ye. Tsedilina; GEOMAGNETIZM I AERONOMIYA, Vol 30 No 5, Sep-Oct 90] 2
Diurnal, Seasonal and Azimuthal Regularities of Backscatter Signals
[O. Alimov, N. P. Marchenko, et al.; GEOMAGNETIZM I AERONOMIYA, Vol 30 No 5, Sep-Oct 90] .. 3

Circuits, Systems

Analytical Determination of Signatures for Multichannel Signature Analyzers
[V. N. Yarmolik, I. V. Kachan; IZVESTIYA VYSSHIKH UCHEBNYKH ZAVEDENIY: PRIBOROSTROYENIYE, Vol 33 No 9, Sep 90] 4
Wideband Frequency Synthesis With Aid of Passive Digital Structures 4
Rise-Time and Amplitude Distortions of Exponential Video Pulses by Electronic Amplifier
[A. I. Inkudinov, V. I. Kravets, et al.; IZVESTIYA VYSSHIKH UCHEBNYKH ZAVEDENIY: PRIBOROSTROYENIYE, Vol 33 No 9, Sep 90] 4
Scattering of Electromagnetic Waves by Reflector Antennas
[Ya. N. Feld; RADIOTEKHNIKA I ELEKTRONIKA, Vol 35 No 8, Aug 90] 5
Use of Ray Trajectories Representations in Extended Parameter Space For Solution of Problem of Wave Propagation Through Nonhomogeneous Media
[Yu. A. Kravtsov, K. V. Sivstunov, et al.; RADIOTEKHNIKA I ELEKTRONIKA, Vol 35 No 8, Aug 90] . 5
Deflection of Light Rays During Multiple Anisotropic Diffraction of Light
[V. B. Voloshinov, B. Traore; RADIOTEKHNIKA I ELEKTRONIKA, Vol 35 No 8, Aug 90] 5
Accuracy of Measurement of Spectral Density of Atmospheric Radio Interference
[D. S. Dobryak, L. G. Petrova; RADIOTEKHNIKA I ELEKTRONIKA, Vol 35 No 8, Aug 90] 6
VLF-ELF Atmospheric Radio Interference as Nonlinear Transformation of Normal Noise
[D. S. Dobryak, Ye. A. Vershinin; RADIOTEKHNIKA I ELEKTRONIKA, Vol 35 No 8, Aug 90] 6
Optimization of Receiver of Phase-Shift-Keyed Pseudorandom Signals in Presence of Worst-Case Interference With Limited Average Power
[A. N. Putilin, Ch. M. Chudnov; RADIOTEKHNIKA I ELEKTRONIKA, Vol 35 No 8, Aug 90] 7

Anisotropically Conducting Helical-Helical Circular Waveguide for Amplifier Stage of Twistron Oscillator
[A. P. Arzin, A. F. Savapin, et al.; RADIOTEKHNIKA I ELEKTRONIKA, Vol 35 No 8, Aug 90] 7
Design Optimization of Single-Mode Optical Fibers Made of Fluoride Glasses For Intermediate-Infrared Radiation
[V. G. Plotnichenko, L. A. Frenkel; RADIOTEKHNIKA I ELEKTRONIKA, Vol 35 No 8, Aug 90] 7
Electron Optical Correlation Methods and Means of Image Recognition: Survey of Literature
[G. I. Vasilenko, I. S. Gibin, et al.; IZVESTIYA VYSSHIKH UCHEBNYKH ZAVEDENIY: RADIOELEKTRONIKA, Vol 33 No 8, Aug 90] 8
Accuracy Analysis of Determination Laser Beam Coordinates in Tracking Television System
[Yu. V. Martyshevskiy; IZVESTIYA VYSSHIKH UCHEBNYKH ZAVEDENIY: RADIOELEKTRONIKA, Vol 33 No 8, Aug 90] 8
Classification of Objects and Scenes With Aid of Correlation Function of Invariant Image Description
[V. V. Dadeshidze, I. N. Kompanets, et al.; IZVESTIYA VYSSHIKH UCHEBNYKH ZAVEDENIY: RADIOELEKTRONIKA, Vol 33 No 8, Aug 90] 9
Radio-Optical Antenna Array With Compression of Long Linear-Frequency- Modulation Signal
[Ye. N. Voronin, I. Yu. Grinev, et al.; IZVESTIYA VYSSHIKH UCHEBNYKH ZAVEDENIY: RADIOELEKTRONIKA, Vol 33 No 8, Aug 90] 9
Output Signal of Adaptive Acoustooptical Processor of Long Linear- Frequency-Modulation Signals
[N. I. Yesepkina, I. P. Lavrov, et al.; IZVESTIYA VYSSHIKH UCHEBNYKH ZAVEDENIY: RADIOELEKTRONIKA, Vol 33 No 8, Aug 90] 10
Statistical Characteristics of Output Signal From Acoustooptical Sum-Difference Phase Meter
[A. Yu. Odintsov; IZVESTIYA VYSSHIKH UCHEBNYKH ZAVEDENIY: RADIOELEKTRONIKA, Vol 33 No 8, Aug 90] 10
Quasi-Optimum Algorithm of Correlational-Extremal Image Processing
[D. I. Bezuglov; IZVESTIYA VYSSHIKH UCHEBNYKH ZAVEDENIY: RADIOELEKTRONIKA, Vol 33 No 8, Aug 90] 10
Image Recognition in Presence of Color Background Interference
[V. K. Baklitskiy; IZVESTIYA VYSSHIKH UCHEBNYKH ZAVEDENIY: RADIOELEKTRONIKA, Vol 33 No 8, Aug 90] 11
Optical Linear-Frequency-Modulation Correlator With Time Integration, Semiconductor Laser, and Charge-Coupled Photodetector
[D. F. Gaynullin, N. N. Yevtikhiyev, et al.; IZVESTIYA VYSSHIKH UCHEBNYKH ZAVEDENIY: RADIOELEKTRONIKA, Vol 33 No 8, Aug 90] 11
Shaping Spatial Radiation Pattern of Transmitter Antenna Arrays With Fibe -Optic Signal Distribution System
[A. N. Bratchikov, A. I. Kukshin, et al.; IZVESTIYA VYSSHIKH UCHEBNYKH ZAVEDENIY: RADIOELEKTRONIKA, Vol 33 No 8, Aug 90] 11
Using Computer for Determining Parameters of Periodic Components of Digital Signals
[V. A. Dvinskikh; METROLOGIYA, No 7, Jul 90] 12
Potential Accuracy of Laser Doppler Velocimeters With Correlation of Photocounts
[A. V. Averkin, A. I. Popov, et al.; METROLOGIYA, No 7, Jul 90] 12
Phase Method of Acoustic Anemometry
[S. Z. Shkundin, V. B. Lashin; METROLOGIYA, No 7, Jul 90] 13

Industrial Electronics, Control Instrumentation

Functional Electronic Element Design Principles
[A. B. Putilin; ELEKTRONNOYE MODELIROVANIYE, No 4, Jul-Aug 90] 14
Design of a Convolution Module to Detect Postulated Class of Defects
[Ye. F. Berezkin, N. V. Yefremov; ELEKTRONNOYE MODELIROVANIYE, No 4, Jul-Aug 90] 14
Improvement of Linear Mathematical-Economics Model to Optimize Structure of Electric Power System Generating Facilities
[A. V. Fomin, L. D. Khabachev, et al.; ELEKTRONNOYE MODELIROVANIYE, No 4, Jul-Aug 90] 14
Use of Analog Relative-Frequency-Difference Converter in Phase Lock Systems
[I. Kh. -G. Korsunskiy; IZMERITELNAYA TEKHNIKA No 7, Jul 90] 14
More Accurate Measurement of Antenna Characteristics on Basis of Apriori Information
[R. I. Rumyantsev; IZMERITELNAYA TEKHNIKA, No 7, Jul 90] 15
Temperature Field in Absorbing Wall of Coaxial Line
[Yu. V. Shpagin, L. G. Martynenko; IZMERITELNAYA TEKHNIKA, No 7, Jul 90] 15
Metrological and Operating Characteristics of Microelectronic QRS- Detectors
[B. I. Podlepetskiy, S. V. Torubarov; IZMERITELNAYA TEKHNIKA, No 7, Jul 90] 15

Electron Devices

Television Image Generators in Radiation Fields 17

Components, Hybrids, Manufacturing Technology

New Generation of Turbogenerators With Air Cooling System
[Ya. B. Danilevich, G. S. Zhuravlev; ELEKTROTEKHNIKA, No 9, Sep 90] 19
Self-Generating Arc Quenchers in SF_6 Circuit Breakers
[L. N. Matkovskaya; ELEKTROTEKHNIKA, No 9, Sep 90] 19
Carbon Slip Rings For A.C. Generators
[A. S. Fialkov, Ye. F. Kolpikova, et al.; ELEKTROTEKHNIKA, No 9, Sep 90] 19
Optimization of K1801VM2-Based Microprocessor Control for Electric Positioning Drive
[V. S. Yudenkov, Yu. V. Lopatin, et al.; ELEKTROTEKHNIKA, No 9, Sep 90] 20
Experience and Problems in Producing Newest Medical Equipment for Mass Use
[V. I. Idasko, A. B. Galitskiy, et al.; ELEKTROTEKHNIKA, No 9, Sep 90] 20

Power Engineering

New Engineering Decisions for Primary Coal Crushing Equipment at Thermal Power Plants
[G. P. Berlyavskiy, B. I. Pasko, et al.; ENERGETIKA I ELEKTRIFIKATSIYA, No 3, Jul-Sep 90] 21
Repair of Low-Voltage Winding Insulation of Power Transformers With Compound Insulators
[V. I. Kostin; ENERGETIKA I ELEKTRIFIKATSIYA, No 3, Jul-Sep 90] 21
Progressive Technology For Manufacture of High-Voltage Insulators
[B. I. Daydash, V. A. Aleko, et al.; ENERGETIKA I ELEKTRIFIKATSIYA, No 3, Jul-Sep 90] 21
Automated PC-Based Workstation For Diagnosis of Oil-Filled Power Equipment
[V. B. Vidzigovskiy, V. A. Kacharov, et al.; ENERGETIKA I ELEKTRIFIKATSIYA, No 3, Jul-Sep 90] 21
Fundamental Concepts for the Future Development of Electric Power Engineering
[L. S. Popyrin; ELEKTRICHESKIYE STANTSII, No 8, Aug 90] 22
Three-Tiered Management Structure For Power Engineering Under Conditions of Complete Cost-Accounting and Self-Financing
[E. F. Makarov; ELEKTRICHESKIYE STANTSII, No 8, Aug 90] 22
Modern 750 kV Power Transmission Lines
[A.N. Sherentsis; ELEKTRICHESKIYE STANTSII, No 8, Aug 90] 22

Industrial Applications

Problems of Autonomous Electric Power Generation and Possible Solutions
[A. I. Lishchenko; TEKHNICHESKAYA ELEKTRODINAMIKA, No 5, Sep-Oct 90] 23
Low-Power High-Voltage Sources
[A. A. Penin; TEKHNICHESKAYA ELEKTRODINAMIKA, No 5, Sep-Oct 90] 23
Automatic Control and Monitoring Device AVTOSHCHIT for Nonconventional Electric Energy Sources
[Ye. V. Shevchenko; TEKHNICHESKAYA ELEKTRODINAMIKA, No 5, Sep-Oct 90] 23

Quantum Electronics, Electro-Optics

Calculation of Calibration Characteristics of Optical Analyzers for Fiber Diameter Measurement Taking Into Account Spectral Characteristics of Radiation Source and of Photodetector
[V. I. Ovod; ZHURNAL PRIKLADNOY SPEKTROSKOPII, Vol 53 No 3, Sep 90] 25
Infrared Radiation Absorption By Ge-Doped Silicon After Neutron Bombardment
[V. V. Borshchenskiy, D. I. Brinkevich, et al.; ZHURNAL PRIKLADNOY SPEKTROSKOPII, Vol 53 No 3, Sep 90] 25
Trends in the Specifications of Series-Manufactured Nonscanning Ultraviolet Spectrophotometers
[B. I. Liflyandchik, A. V. Maliy; OPTIKO-MEKHANICHESKAYA PROMYSHLENNOST, No 8, Aug 90] 25
Nonhomothetic Transformation of a Background Interference Domain in Multispectrum Systems With Different Fields
[Yu. P. Safronov; OPTIKO-MEKHANICHESKAYA PROMYSHLENNOST, No 8, Aug 90] 26
Investigation of Wavefront Restoration Accuracy by Interferogram Processing
[M. A. Gan, S. I. Ustinov, et al.; OPTIKO-MEKHANICHESKAYA PROMYSHLENNOST, No 8, Aug 90] 26

Recording of Lateral Shear Holographic Interferograms By Spatial Filtering
[V. G. Gusev; OPTIKO-MEKHANICHESKAYA PROMYSHLENNOST, No 8, Aug 90] 26
Determination of Spherical Surface Errors By Spherical Beam Interferometry
[V. B. Gubin, V. N. Sharonov; OPTIKO-MEKHANICHESKAYA PROMYSHLENNOST, No 8, Aug 90] 26

Daylighting-90 International Conference

917K0039A Moscow SVETOTEKHNIKA in Russian No 10, Oct 90 p 1

[Article by Unsigned]

[Abstract] An announcement is presented in Russian and English for the International Conference Daylighting-90, to be held October 9-12 at the Scientific-Research Institute of Structural Physics. The conference will involve participants from the USSR, USA, Czechoslovakia, Japan, Sigapore, France and other nations. Over 100 reports on different aspects of research in the field of daylighting and combined lighting will be presented at the planery meeting and in four sections. This special issue of Svetotekhnika contains some of the papers to be presented at the conference.

UDC 628.9.021—535.625.2:311.17

Analysis of Sky Brightness Distribution Models

917K0039B Moscow SVETOTEKHNIKA in Russian No 10, Oct 90 pp 5-8

[Article by R. Kittler, L. Pirshel, Slovak Academy of Sciences, Bratislava]

[Abstract] Various analytic sky models have been created considering the mean weighted interactions of the basic atmospheric and solar lighting effects. An empirical method has also been used to create sky brightness models, allowing the combination of a sufficient representative quantity of measured data thus producing a model of the sky by the use of methods of approximation attempting as a result to obtain the distribution of brightness best corresponding to nature. The analytical, statistical and combined models of the distribution of brightness in the sky are compared. Samples of brightness distribution models generated by computer graphics methods are presented. Figures 4.

UDC 628.921/.928

The Brightness of the Urban Environment

917K0039C Moscow SVETOTEKHNIKA in Russian No 10, Oct 90 pp 9-11

[Article by V. D. Bakharev, L. N. Orlova, Gorkiy Construction Engineering Institute imeni V. P. Chkalov]

[Abstract] The luminance in rooms located in the lower storage of buildings shielded by surrounding structures depends on the brightness of the Earth and segments of other buildings visible through lighting passages. This article calculates the luminance factors and brightness of building facades, assuming that all surrounding surfaces reflect light according to Lambert's law. The model of brightness of the urban environment is intended for theoretical studies of systems of natural lighting for rooms with lateral illumination. Figures 5; References 5: Russian.

UDC 628.925.2

Light-Transmitting Elements of Polymethyl Methacrylate and Polycarbonate

917K0039D Moscow SVETOTEKHNIKA in Russian No 10, Oct 90 pp 12-14

[Article by U. Fisher, Germany]

[Abstract] The first successful tests of polymethyl methacrylate (PMMA) and polycarbonate (PC) as greenhouse construction materials, undertaken in the USSR, stimulated the writing of this article, intended to familiarize designers with the properties of these materials. Examples of architectural uses of the materials are presented in photographs. Recommendations are given for manufacture, transportation, storage and installation of the materials. Figures 8.

UDC 628.921

Engineering Method of Designing Natural Illumination Systems for Rooms With Effective Sun Protection

917K0039E Moscow SVETOTEKHNIKA in Russian No 10, Oct 90 pp 16-19

[Article by M. Yu. Mitnik, A. V. Spiridonov, Scientific Research Institute of Construction Physics]

[Abstract] Experimental studies were used to determine the distribution of the natural lighting utilization factor for various natural lighting systems with fixed mutual placement of the Sun and the light passage considered. The authors have developed a program for the design of three-dimensional surfaces, intended to be run on personal computers. The program can construct cross sections of three-dimensional surfaces, the points of which are fixed in a rectangular coordinate grid. The program computes thermal inputs to rooms for various surroundings of the building, various types of Sun-protection devices and orientations of building surfaces and Sun angles. Figures 4; References 6: 4 Russian, 2 Western.

Model of Variations in the Electronic Density Profiles of the Polar Ionospheric D-Layer as a Function of Riometric Absorption

917K0040A Moscow GEOMAGNETIZM I AERONOMIYA in Russian Vol 30 No 5, Sep-Oct 90 pp 788-791

[Article by L. V. Zelenkova, V. A. Soldatov, V. F. Laykova]

[Abstract] The relationship between the electronic density profile in the ionospheric D-layer in polar regions and the riometric absorption level as well as magnetic field variations is investigated. Expressions are derived that make it possible to obtain the differential flux of incoming electrons responsible for such absorption for each riometric absorption level. Extensive experiemental data on altitude profile variations were used to calculate the altitude distribution of the electron concentrations at high altitudes. These calculations made it possible to record variations in the electronic density profile accurate to a factor of two depending on the degree of ionospheric disturbances. The four-parameter technique for describing the electronic density profile proposed here accurately reflects changes in the electronic concentration from ionospheric disturbances.

UDC 550.388.2

Estimation of E-Layer Parameters From Long-Range Oblique Sounding Data

917K0040B Moscow GEOMAGNETIZM I AERONOMIYA in Russian Vol 30 No 5, Sep-Oct 90 pp 793-798

[Article by R. Martin, L. Palasio, A.V. Popov, Yu.N. Cherkashin]

[Abstract] A quasiparabolic single-layered ionospheric model is used to obtain a simple estimate of the critical frequency and geometric parameters of the ionospheric F-layer. In this technique the maximum frequencies of the individual wave propagation modes and relative signal delays are the only data recovered from the ionograms. The analysis results are presented in convenient nomogram form. The horizontal gradients are accounted for by means of an adiabatic approximation. The critical frequencies and ionospheric base altitudes predicted by the model are in good agreement with long-term ionospheric forecasting data for the Moscow-Havana route.

UDC 550.388.2

Propagation Features of Low-Frequency Electromagnetic Disturbances Caused by Ionospheric E-Layer Excitation

917K0040C Moscow GEOMAGNETIZM I AERONOMIYA in Russian Vol 30 No 5, Sep-Oct 90 pp 806-812

[Article by V.V. Surkov]

[Abstract] The space-time distribution of geomagnetic disturbances caused by the nonmonotonic nature of a derived dispersion relation is investigated employing a sample concentrated source. This analysis is based on the common propagation features of natural low frequency (0.1 to 1 Hz) electromagnetic oscillations of the ionospheric E-layer. Primary attention is given to the fundamental mode which has the most severe attenuation near the spectral maximum. The solution is obtained as a series that sums the contributions of the individual natural oscillations in this layer. It is determined that far from the source the characteristic scale of the excitation grows due to dispersion, while its maximum travels at a near-constant velocity corresponding to the group velocity of the fundamental mode near the attenuation minimum.

UDC 550.388.2

Global Ionospheric Disturbances Generated by the Electrical Field From the "Morskaya Zvezda" Atomic Explosion on July 9, 1962

917K0040D Moscow GEOMAGNETIZM I AERONOMIYA in Russian Vol 30 No 5, Sep-Oct 90, pp 813-819

[Article by Ye. Ye. Tsedilina, V. M. Shashun'kina]

[Abstract] Previously-reported theoretical calculations of the electrical field generated by the "Morskaya Zvezda" Atomic Explosion on July 9, 1962 are used to determine the far-field terrestrial region that will contain a powerful electrical field as a result of such an explosion. It is demonstrated from an analysis of the electrical field calculations and estimates of its effect on charged particle concentrations in the atmosphere that substantial ionospheric disturbances of approximately twenty percent should be observed within this region; such results have not been previously reported in the literature. These characteristic theoretically- predicted features of the ionospheric disturbances can be used for identification and proper interpretation of such disturbances.

UDC 550.388.2

Global Ionospheric Perturbations Caused by the Electrical Field From the "Morskaya Zvezda" Atomic Explosion of July 9, 1962. Part II

917K0040E Moscow GEOMAGNETIZM I AERONOMIYA in Russian Vol 30 No 5, Sep-Oct 90 pp 820-825

[Article by Ye. Ye. Tsedilina, V. M. Shashun'kina]

[Abstract] The ionospheric field disturbances caused by the electrical pulse generated by the "Morskaya Zvezda" atomic explosion of July 9, 1962 are analyzed based on data provided by six ionospheric monitoring stations around the world. Ionospheric data plots in the region of strong field effects from monitoring stations in Churchill, Kenora, Ottawa, St. Johns, White Sands, and Mexico are provided

together with similar plots for stations in South America. These data reveal a strong explosion-generated electrical field effect on the ionosphere. It is demonstrated that in the initial instant following the blast the electron concentration in the ionospheric E-layer drops by approximately twenty percent in the strong electrical field range, while the entire layer diminishes overall as well.

UDC 550.388.2

Diurnal, Seasonal and Azimuthal Regularities of Backscatter Signals

917K0040F Moscow GEOMAGNETIZM I AERONOMIYA in Russian Vol 30, No 5, Sep-Oct 90 pp 826-831

[Article by O. Alimov, N. P. Marchenko, L. N. Rubtsov, I. A. Tushentsova, Ye. Ye. Tsedilina]

[Abstract] Diurnal, seasonal and azimuthal regularities of backscatter signals are investigated based on experimental azimuthal scanning radar backscatter signals at 20 MHz obtained in Dushanbe (38 degrees N, 68 degrees E) from April 1987 through January of 1988. The instrumentation and measurement technique used in these studies are described. The dependences of the averaged minimum and maximum group path of the backscatter signals as a function of time of day and season in Dushanbe are provided together with a plot of the seasonal progression of the median maximum reflection frequencies off the ionospheric E-layer for the case of vertical incidence. The year-long observation period in Dushanbe was found to substantially improve the accuracy of radiowave predictions. An analysis of these experimental data can be used to relate the ionospheric dynamics and reflecting surface relief to the features of backscatter signals arriving from different azimuthal angles.

UDC 681.325.65

Analytical Determination of Signatures for Multichannel Signature Analyzers

917K0060A Leningrad IZVESTIYA VYSSHIKH UCHEBNYKH ZAVEDENIY: PRIBOROSTROYENIYE in Russian Vol 33 No 9, Sep 90 pp 33-38

[Article by V. N. Yarmolik and I. V. Kachan, Minsk Institute of Radio Engineering]

[Abstract] An analytical method of calculating signatures for the most common versions of multichannel signature analyzers is outlined, two such analyzers being one with an internal modulo-2 adder and another one being the Built-In Logic Block Observation analyzer. The calculation is based on the system of two equations describing the analyzer operation and on its characteristic polynomial. A matrix is shown to exist which relates the states of a given multichannel signature analyzer. A formula for the signatures is obtained which derives from the linearity of the modulo-2 summation operation. Figures 2; references 6.

UDC 621.373

Wideband Frequency Synthesis With Aid of Passive Digital Structures

917K0060B Leningrad IZVESTIYA VYSSHIKH UCHEBNYKH ZAVEDENIY: PRIBOROSTROYENIYE in Russian Vol 33 No 9, Sep 90 pp 39-47

[Article by Yu. A. Nikitin, Leningrad Institute of Electrical Communications Engineering imeni Professor M.A. Bonch-Bruyevich]

[Abstract] Eight structures of finite digital automatons most suitable for two-level passive frequency synthesis, namely for division of a reference frequency f_0 by a fractional number $N = P/Q$ to obtain an output frequency f_A, are comparatively evaluated in terms of frequency ratio, mean-square error of the quasi-uniform pulse sequence over the nonuniformity period, and coupling to a controllable inhibit circuit. Six of these automatons are based on an accumulator register, the first three being direct-frequency automatons controlled by the direct code Q of the output frequency f_A. Although their output frequencies are each based on the same relation to the reference frequency, these three automatons differ with respect to duration nonuniformity of pulses in the sequence and necessary accumulator speed. The fourth automaton is similar to the first one, but with additional control by another code. The last two of those six automatons can synthesize a grid of frequencies or a grid of periods, each mode of operation requiring a different number Q at the accumulator register input and a different adder capacity P. The seventh, a direct-period automaton, is based on a variable divisor and synthesizes a grid of periods directly proportional to the control code N = integer + fraction. Synthesis of a frequency grid by this automaton requires addition of a code calculator which will divide the reference frequency f_A by N = whole part of $P/Q + \alpha/Q$ ($\alpha = 0,1,...,Q-1$). The eighth automaton is based on a fractional-variable divisor for frequency synthesis according to Euclid's algorithm, with the divisor N in the form of a continued fraction. This automaton, controlled by a fixed- capacity accumulator register, is the one most easily coupled to a linear precisely adjustable inhibit circuit. The highest reference frequency for such an automaton is determined principally by the accumulator register speed, its highest possible output frequency being determined by the code divider speed and word length. Both seventh and eighth automatons will synthesize, without additional hardware, a grid with the same given quality indicators but covering a wider frequency range or a grid covering the same frequency range but having better quality indicators when interfaced with a control computer (central processor) or a built-in microcomputer. Figures 3; references 14.

UDC 621.317.741:621.372.512.029.33

Rise-Time and Amplitude Distortions of Exponential Video Pulses by Electronic Amplifier

917K0060C Leningrad IZVESTIYA VYSSHIKH UCHEBNYKH ZAVEDENIY: PRIBOROSTROYENIYE in Russian Vol 33 No 9, Sep 90 pp 59-64

[Article by A. I. Ankudinov, V. I. Kravets, K. A. Ankudinov, and V. P. Kodorchenko, Leningrad]

[Abstract] Transformation of an exponential video pulses during its passage through an electronic amplifier is analyzed, considering that such an amplifier consists of lumped-parameter and distributed-parameter active and passive elements. The transfer function of such an amplifier is reduced to $W_l(s) = s\tau_l K/(1+ s\tau_l$ in the low-frequency range and $W_h s = K/(1+ s\tau_h$ in the high-frequency range, $W(s) = s\tau_l K/(1+ s\tau_l)(1+ s\tau_h)$ covering the entire frequency range (τ being the respective time constants). A signal of the form $v_{in}(t) = V_{in}e^{-t/\tau}$ with a time constant τ is considered at the amplifier input. The output signal V_{out} is calculated by the method of Laplace transforms, constants being generally different. The calculations are simplified by first assuming that the signal time constant is equal successively to the two amplifier time constants. The changes in signal rise time and relative amplitude are then characterized by the index $\delta = |(V_{out} - KV_{in})/KV_{in}|$ which relates the output signal to the input signal. Both changes are normalized and as such calculated for given signal time constant τ and ratio of the amplifier time constants $m = \tau_l/\tau_h$, this ratio being equal to the ratio f_h/f_l of upper cutoff and lower cutoff frequencies. These two frequencies can then also be readily determined. The algorithm has been programmed on an Elektronika DZ-28 microcomputer. The results of calculations for an amplifier with $f_l = 60$ Hz and $f_h = 60$ kHz agreed within +/- 5 percent with test results. Figures 2; tables 1; references 8.

UDC 621.396.67.01

Scattering of Electromagnetic Waves by Reflector Antennas

917K0037A Moscow RADIOTEKHNIKA I ELEKTRONIKA in Russian
Vol 35 No 8, Aug 90 pp 1596-1603

[Article by Ya. N. Feld]

[Abstract] Scattering of a plane electromagnetic wave by a reflector antenna in the form of a truncated paraboloid of revolution with linear dipole at the focus perpendicular to the axis is analyzed, assuming that the reflector is infinitesimally thin and an ideal conductor. The dipole is connected to an impedance and a primary wave E^0,H^0 impinges on the reflector surface, that surface being fictitiously complemented to a geometrically closed one and a family of appropriate auxiliary currents being stipulated on the entire surface. The vector function is determined which represents the current density on the physical metal surface and the tangential component of the electric vector on the complementary geometrical surface, with the aid of its Fourier coefficients is then constructed a convergent series each term of which satisfies the Meixner boundary conditions at the reflector edge. The reflector current is calculated next and then are calculated the scattered field and the scattering cross-section of the reflector. Figures 2; references 5.

UDC 537874.4.01

Use of Ray Trajectories Representations in Extended Parameter Space For Solution of Problem of Wave Propagation Through Nonhomogeneous Media

917K0037B Moscow RADIOTEKHNIKA I ELEKTRONIKA in Russian
Vol 53 No 8, Aug 90 pp 1603-1609

[Article by Yu. A. Kravtsov, K. V. Svistunov, and M. V. Tinin]

[Abstract] Propagation of waves through a two-dimensionally nonhomogeneous medium from a point source in this medium is analyzed by using the representation of ray trajectories in an extended parameter space, a typical medium under consideration being the Earth's ionosphere. The conventional (x,z)-space is accordingly "unfolded" into one with the angle of departure as the third parameter-coordinate. Calculations made on this basis pertaining to propagation of radio waves along the Khabarovsk-Irkutsk return route are shown to yield much clearer results, in terms of graphical resolution, than do calculations based on the conventional representation of trajectories in the (x,z) plane. The same concept is subsequently applied to construction of integral caustic short-wave asymptotes, using an interference integral somewhat different than Yu.I. Orlov's (TRUDY MOSKOVSKOGO ENERGETICHESKOGO INSTITUTA No 119, 1972). As a specific problem is considered the two-dimensional field of a point source describable by the Helmholtz equation, this field being a function not only of the space coordinates x,y but also depending on the x_0 coordinate of the source. Solution of this problem by the "partial" field method, using the Fourier integral with respect to the third parameter $s = \cos\beta$ (β_0- angle of departure) and with the Helmholtz equation modified accordingly, yields the field in the ray representation with an amplitude and a phase which satisfy the conventional equation of geometrical optics. For a determination of the partial wave are then needed trajectories which depart from the $z = 0$ plane at angle β_0 and arrive at the observation point (x,z). Figures 5; references 10.

UDC 537.874.6

Deflection of Light Rays During Multiple Anisotropic Diffraction of Light

917K0037C Moscow RADIOTEKHNIKA I ELEKTRONIKA in Russian
Vol 35 No 8, Aug 90 pp 1610-1616

[Article by V. B. Voloshinov and B. Traore]

[Abstract] Multiple anisotropic Bragg diffraction of light by two acoustic waves of equal or nearly equal frequencies propagating in mutually orthogonal directions through a crystal is analyzed, assuming that the crystal is a uniaxial positive optical one the two acoustic waves propagate in a plane perpendicular to its optical axis. The resulting deflection of light rays is calculated on the basis of a system of coupled differential equations for plane light waves and their interaction with ultrasound, the intensity of light in the diffraction orders and thus efficiency of light in each depending on the power of the acoustic waves. Eight scattering-intensity maxima are shown to be attainable, but the acoustic power being too high compared with the power for single scattering. An experiment was performed with a paratelluride TeO_2 crystal, this crystal being characterized by a large value of the M_2 acoustooptic interaction index. Light in this and any medium is multiply diffracted by acoustic waves within a very narrow frequency band and such a diffraction requiring precise tuning of the optical system. With $M_2 = 1200 \times 10^{-18}$ s^3/g, the acoustic frequency for diffraction of 633 nm light in this crystal is $f_0 = 38$ MHz. In this experiment the light beam of a He-Ne laser passed through a mechanical beam chopper, a polarizer, a quartz polarization plate, and a diaphragm into the paratelluride crystal acting as an acoustooptic cell with the optical axis in the [001] direction, the angle of

incidence being read on the goniometer scale in front of the crystal. Two piezoelectric transducers were glued onto the cubic cell, one onto each of two adjacent lateral faces, one a $LiNbO_3$ crystal and one a quartz crystal, for emission of acoustic waves in [110] and [110] directions respectively. Electric signals from two high-frequency power oscillators were converted by these transducers into traveling acoustic waves in the form of 3-5 μs pulses with repetition rate of 1000 Hz. Light rays deflected by these waves were, after passage through a photomultiplier, recorded on an oscillograph. The results of this experiment confirm the theoretical ones qualitatively, a maximum diffraction efficiency of 40 percent having been reached in the fourth (65 percent theoretically) and of 10 percent having been reached in the other seven orders. Figures 5; references 8.

UDC 551.511.6.001.573

Accuracy of Measurement of Spectral Density of Atmospheric Radio Interference

917K0037D Moscow RADIOTEKHNIKA I ELEKTRONIKA in Russian
Vol 35 No 8, Aug 90 pp 1630-1635

[Article by D. S. Dobryak and L. G. Petrova]

[Abstract] Measurement of the spectral density of atmospheric radio interference is analyzed for accuracy, this interference being a non-Gaussian nonstationary one. The analysis is based on the model of ELF-VLF interference as an additive mixture of two components, fluctuation noise and a flux of random stray pulses. Measurement of the spectral density of atmospherics for a given frequency is considered and the attendant error due to finiteness of the measuring time is of concern, the measuring time being usually not shorter than 1 s and sufficiently long for an approximately Poisson distribution of stray fluxes with a Poisson distribution of pulses within each flux but necessarily not longer than the correlation time so that regular diurnal variation can be disregarded. Inasmuch as the autocorrelation function covers a time interval of a few milliseconds only, the error of its estimation can also be disregarded. The correlation time is frequency dependent and the spectral density of atmospherics depends on their flux intensity, both the intensity of those exceeding the threshold level for a given frequency and lightning discharges occurring worldwide within a given period of time needing to be included. The measuring problem is formulated as one of estimating the magnitude of a constant signal which appears with both a stationary "white" noise and a nonstationary "color" noise, each noise characterized by linearly decreasing dispersion. The frequency-dependent minimum attainable measurement error and the therefore also frequency-dependent optimum measuring time for attaining this ultimate accuracy are calculated analytically and then numerically, with the aid of experimental data, taking into account both hourly and seasonal variations. In winter without thunderstorms occurring in the vicinity, the measuring time for the 0.3-6.0 kHz frequency range should be made equal to the correlation time, inasmuch as the true optimum measuring time would be longer. In summer the optimum measuring time for the entire 0.02-20 kHz frequency range does not exceed 20 min, the maximum accuracy reaching 35 percent at the 2.5 kHz frequency but only about two percent at both 20 Hz and 20 kHz frequencies with an optimum measuring time of 3.3 min for the latter. Figures 2; references 8.

UDC 551.511.6.001.573

VLF-ELF Atmospheric Radio Interference as Nonlinear Transformation of Normal Noise

917K0037E Moscow RADIOTEKHNIKA I ELEKTRONIKA in Russian
Vol 35 No 8, Aug 90 pp 1635-1641

[Article by D. S. Dobryak and Ye. A. Vershinin]

[Abstract] A model of atmospheric radio interference is constructed by nonlinear transformation of normal noise, a sinh nonlinearity most closely satisfying the requirement of a linear trend as the value of the argument approaches zero and an exponential trend as its value approaches the maximum. A multidimensional distribution of the $u(t) = U \sinh \gamma x(t)$ process is considered, assuming that this process is the transform of a normal $x(t)$ process with unity dispersion and that the transformation is inertialess. The relations between the autocorrelation functions of the two processes is established accordingly, on the basis of two samples. The mean number of upward threshold crossovers by the overshoot flux intensity and the distribution of overshoot amplitudes are then calculated, taking into account the monotonicity of that transformation. The parameters of the atmospherics distribution are estimated not on the basis of maximum likelihood, which involves solving a system of transcendental equations very difficult to simulate in the analog mode, but on the basis of several measurements of the overshoot flux intensity v at different threshold levels E including the zero level. The other levels should not be higher than the one at which $v(E) = v(0)e^{0.032}$, considering that the distribution parameter γ is not larger than 1.5 and the overshoot flux intensity therefore never exceed that threshold. This procedure in the one-dimensional formulation is consistent with experimental data according to the chi-square criterion, the vertical component of 0.07-1 kHz electromagnetic fields been recorded on magnetic disks. The validity of the proposed model of atmospheric radio interference in the two- dimensional formulation has been confirmed, also according to the chi-square criterion, on the basis of a 0.81 correlation coefficient for paired samples of both processes with samples from different pairs remaining mutually independent. Figures 3; references 7.

UDC 621.391.01

Optimization of Receiver of Phase-Shift-Keyed Pseudorandom Signals in Presence of Worst-Case Interference With Limited Average Power

917K0037F Moscow RADIOTEKHNIKA I ELEKTRONIKA in Russian Vol 35 No 8, Aug 90 pp 1646-1650

[Article by A. N. Putilin and Ch. M. Chudnov]

[Abstract] The problem of optimizing a receiver of PSK pseudorandom signals for maximum interference immunity is tackled, considering worst-case interference with limited average power. The sender consists of sources of binary messages connected in series and followed by a modulator which forms pseudorandom signals. The receiver on the other end of the transmission line is preceded by a demodulator with limitation threshold B. The problem of signal processing is formulated in terms of a game for the asymptotic case of signal and interference sampling base n approaching infinity, the total signal at the demodulator input being the sum of the useful one S and an interference with an unknown distribution. Its worst distribution is the one corresponding to the maximum probability of reception error at a given relative demodulator limitation threshold $\beta = B/S$, whereupon the optimum decision rule is established accordingly. The optimum relative limitation threshold is determined next, assuming that it is proportional to n^{α}. Insertion of a limiter with $\alpha \geq 1$ or $\alpha \leq 1/2$ is shown not to raise the guaranteed interference immunity of reception, the maximum interference immunity being guaranteed by insertion of limiter with α within the 0.5-1 range. References 9.

UDC 621.385.69

Anisotropically Conducting Helical-Helical Circular Waveguide for Amplifier Stage of Twistron Oscillator

917K0037G Moscow RADIOTEKHNIKA I ELEKTRONIKA in Russian Vol 35 No 8, Aug 90 pp 1688-1691

[Article by A. P. Arzin, A. F. Sayapin, and Yu. G. Shteyn]

[Abstract] A helical circular waveguide shaped into a helix is described, such a structure having been designed for the amplifier stage of twistron oscillators which convert the energy of a relativistic high- current short-duration electron beam into microwave energy. The principle of its operation is based longitudinal interaction of beam electrons and E_{0m}-mode waves without transformation of the latter into H_{1m} and E_{1m} waves, which takes place in a plain circular waveguide with the same cross-section, and thus with neither the interaction efficiency being lowered nor the oscillation mechanism being distorted. Mode transformation in this helical-helical waveguide is suppressed by suppression of azimuthal current conduction. To achieve this, the waveguide is made up of separate wires connected to dielectric rings and the latter are fastened with screws alternately along four quadrature directrices. Both the period of this structure and the radius of the center line are adjustable. Leads are brought out from both end rings to the center so as to ensure matched excitation and facilitate extraction of microwaves. In the first experiments with such a structure current pulses of nanosecond duration were converted into 4.2 cm microwave radiation and, in single-mode operation, into 3.7 GHz or 10 GHz microwave radiation. The radiation pattern of this oscillator and the dispersion characteristic of its amplifier operating with a tubular relativistic electron beam were subsequently measured in the LUCH ("Ray") accelerator, the nominal amplitudes of voltage and 120 ns current pulses being 1.5 MV and 20 kA respectively. No self-excitation of the structure occurred during formation of a tubular electron beam by a magnetically shielded diode in a leading magnetic field of up to 2 T intensity. The velocity of this beam was then modulated by the circularly polarized electric field of the E_{110}-mode wave during subsequent passage through a adjustable-length cylindrical resonator. Density bunching of the electron beam took place in the helical-helical waveguide, where it also interacted with the traveling wave it had generated. The resonator cavity with movable end walls for varying its length from 4 cm to 12 cm had been designed for self-excitation at an approximately 3 GHz critical frequency for the E_{110} mode. The far-field radiation pattern was found to have the maximum always along the axis and the pulseform of the output signal always duplicated that of oscillations generated in the resonator cavity, evidence of a linear amplification characteristic. Exact synchronism of electrons with a relative velocity $\beta = 0.94$ and the E_{01}-mode wave in a waveguide with an irregularity factor $\nu = [1+(2\pi\rho/h)^2]^{1/2} = 1.15$ (ρ,h- radius and period of center line) was attained for a radiation of approximately 8 cm wavelength. Figures 3; tables 1; references 4.

UDC 537.876.4

Design Optimization of Single-Mode Optical Fibers Made of Fluoride Glasses For Intermediate-Infrared Radiation

917K0037H Moscow RADIOTEKHNIKA I ELEKTRONIKA in Russian Vol 35 No 8, Aug 90 pp 1730-1738

[Article by V. G. Plotnichenko and L. A. Frenkel]

[Abstract] Inasmuch as the spectral characteristics of the refractive index and of the material dispersion determine the design of an optical fiber and particularly the profile of its refractive index needed for maximum data transmission speed, single-mode optical fibers made of fluoride glasses have been considered for operation at intermediate-infrared wavelengths. As the design criterion is selected zero first-order chromatic dispersion at two or more wavelengths. The design procedure is applied to fibers made of

ZBLA glass (Zr,Ba,La,Al fluorides) for zero chromatic dispersion at two wavelength λ_{01},λ_{02}: 1) 2.2 μm and 2.5 μm, 2) 2.5 μm and 3.5 μm, 3) 2.2 μm and 3.5 μm. With a profile of the refractive index $n(r) = n_1(1 - \Delta(r/a)^\alpha$ where $r < a$ and $n(r) = n_1(1 - \Delta)$ where $r \geq a$ (n_1- maximum refractive index, $\Delta = (n_1 - n_3)/n_1$ - relative difference between refractive indexes, n_3- refractive index of sheath material, b- radius of core, r- radial coordinate in a cylindrical system), zero chromatic dispersion at any of those three pairs of wavelengths is attainable in a ZBLA fiber but not at both 1.3 μm and 1.55 μm wavelengths in a quartz fiber. An analysis of the attenuation characteristic reveals that attenuation due to intrinsic losses in the glass as well as attenuation due to irregularities in the fiber (additional Rayleigh scattering by alloy impurities in the core, splices joining fiber segments, microbends) depends, as in a quartz fiber, on the size of the spot representing the lowest-order mode. Calculations made for ZBLA glass doped with GeO_2, 1 km long fiber segments joined by splices, and microbends with a Gaussian spectral distribution of curvature indicate ways to minimize the total losses and the optimum range of spot size. The correlation length being $L \approx b(E_c/E_3)^{1/4}$ (b- outside radius of fiber, E_c,E_3- moduli of elasticity of core material and of sheath material respectively), that ratio of moduli of elasticity can be decreased by either increasing the outside radius or by coating the sheath with a material whose modulus of elasticity is close to that of the core material. The authors thank V.I. Volman, Ye.M. Dianov, and A.S. Kurkov for helpful discussions. Figures 5; tables 3; references 17.

UDC 621.391:535.4

Electron Optical Correlation Methods and Means of Image Recognition: Survey of Literature

917K0062A Kiev IZVESTIYA VYSSHIKH UCHEBNYKH ZAVEDENIY: RADIOELEKTRONIKA in Russian Vol 33 No 8, Aug 90 pp 15-27

[Article by G. I. Vasilenko, I. S. Gibin, O. I. Potaturkin]

[Abstract] Optical and electron optical methods and means of image recognition are surveyed, covering the entire image recognition process from image perception through field transformation for determination of image parameters to logic operations and the decision mechanism. Systems based on scanning the members of a class and comparing each with a standard are the most fundamental ones but requiring information about the distribution function. Other systems are based on commonality of characteristics or on clusterization. Methods not requiring information about the distribution functions include discriminant analysis and the ranking algorithm. The best results under conditions of a'priori indeterminacy are obtained by these two methods, but both require lengthy computation procedures and intricate circuitry. Another alternative is the method of admissible transformations, which involves testing hypotheses with respect to the likelihood criterion in a way similar to the optimum Bayes procedure and in which the correlation function serves as the congruence criterion when the distribution functions approximate a multidimensional normal law. Preliminary image processing involves detection of the image contour, either by emphasis of luminance dips with the aid of a spatial operator (Laplace, Roberts, Sobel) and subsequent amplitude limitation or by contour approximation. Obtaining a "gradient" contour requires noise suppression, for which a median filter is most suitable. Inasmuch as image processing is most often done under widely varied rather than rigidly fixed conditions, isomorphic transformation has become a must. Correlators for such a transformations are generally based on principles of geometrical or physical (diffraction) optics, a special group being sequential correlators with photodetector shift registers which continuously process data electrically along one space coordinate and optically along the other. An important advance are holographic correlators: linear amplitude correlators (Vander Lugt and subsequent modifications), a dynamic holographic amplitude correlator with mutually modulated Fourier transforms using a spatial real-time light modulator on a MOS-LC structure (MOS = metal-oxide-semiconductor, LC = liquid crystal) as reversible recording medium, and a holographic intensity correlator using a cathode-ray tube. The intensity correlator features spatial invariance during parallel and multichannel high-resolution image processing, moderate adjustment precision requirements, and insensitivity to phase distortions, but cannot produce an alternating pulse response so that it may have to be replaced with an acoustooptic deflector or modulator. A two-dimensional correlation function for integration in both space and time can be obtained by continuous integration with respect to one space coordinate (x) and summation over n, this summation being effected by time integration in a detector with time delay and storage. References 64.

UDC 681.783.25

Accuracy Analysis of Determination Laser Beam Coordinates in Tracking Television System

917K0062B Kiev IZVESTIYA VYSSHIKH UCHEBNYKH ZAVEDENIY: RADIOELEKTRONIKA in Russian Vol 33 No 8, Aug 90 pp 34-38

[Article by Yu. V. Martyshevskiy]

[Abstract] Determination of the laser beam coordinates in a tracking television system is analyzed for accuracy, considering that the parameters of the useful signal and of the beam trajectory vary. The analysis is based on the Markov theory of optimum nonlinear filtration. The television image converter reads data frame-by-frame into a two-dimensional NxN array of discrete video

signal readings, the laser beam being tracked by processing the video signal in a two-dimensional LxL strobe (L < N). The converter output signal is represented as the sum of useful signal and background noise. The laser beam trajectory in the X,Y plane (X- frame coordinate, Y- line coordinate) is represented as the sum of a quasi-determinate component and a random component along each coordinate. In the state space it is described by the differential equation dX/dt = FX(t)+ GN(t) relating the the vector of variable states X(t) to the partitioned matrix F of system states and the partitioned matrix G of perturbation noise. Calculations were made on a computer by the method of direct probabilistic simulation with all relevant quantities normalized to a frame time of 20 ms, the frame field having been discretized into 256x256 elements and time having been discretized into 0.25 μs intervals. The luminance distribution on the detector surface was assumed to be a Gaussian one, with the image dimension equal to four or five elements at the 1/e level and the strobe dimensions ranging from eight to 10 elements. The simulation procedure involved 200 statistical tests and averaging of the data. An analysis of the results indicates that, with the laser beam moving at the same velocity along both X and Y coordinates, the error of frame coordinate determination is 1.5-2 times larger than the error of line coordinate determination. The simulation algorithms were found to be not only stable in time but also robust with respect to inaccuracy of signal model parameters and laser beam dynamics, a 20-25 percent deviation of the beam spot dimensions from nominal ones increasing the dispersion of the coordinates determination error by only three-five percent. Figures 2; references 3.

UDC 681.142.65.778.39

Classification of Objects and Scenes With Aid of Correlation Function of Invariant Image Description

917K0062C Kiev IZVESTIYA VYSSHIKH UCHEBNYKH ZAVEDENIY: RADIOELEKTRONIKA in Russian Vol 33 No 8, Aug 90 pp 38-44

[Article by V. V. Dadeshidze, I. N. Kompanets, G. A. Lunyakova, A. A. Vasilyev, and S. N. Vereskov]

[Abstract] A method of classifying objects and scenes with the aid of a cyclic correlation function is proposed, the location of an object in a being determined during segmentation of the latter. Each object in that scene is, moreover, described by a set of indicator invariant with respect to scale and orientation. The procedure involves comparing the original with its geometrical transform by using data on local maxima and by seeking their center of gravity or, in the case of more than one object in a scene, seeking connected regions. This method of determining the coordinates of an object in a scene was experimentally implemented with a dynamic holographic correlator and a He-Cd laser, the latter followed by a beam widener, two beam splitters, and an objective lens. The procedure involved simultaneous Fourier transformation of the original and its transform, a negative with the letters S and N serving as the original scene. As dynamic hologram used an optically controllable spatial real-time light modulator of the liquid-crystal photodetector kind with a 90 percent Se + 10 percent As semiconductor layer. Subsequent correlational comparison of some image parts with others will yield the necessary image indicators which are invariant with respect to scale and orientation, most conveniently in the form of a vector, for all objects of any shape in a scene rather than only for objects of symmetric shapes only. Figures 4; tables 2; references 11.

UDC 621.396.677.621.373.826(024)

Radio-Optical Antenna Array With Compression of Long Linear-Frequency- Modulation Signal

917K0062D Kiev IZVESTIYA VYSSHIKH UCHEBNYKH ZAVEDENIY: RADIOELEKTRONIKA in Russian Vol 33 No 8, Aug 90 pp 45-51

[Article by Ye. N. Voronin, A. Yu. Grinev, and A. A. Rymov]

[Abstract] An acoustooptical processor based on a correlator with spatial integration with standard acoustooptic light modulators for linear antenna arrays is described which compresses linear-frequency-modulation signals of duration $\Delta T \leq M\tau_{AOM}$window ($\tau_{AOM}$- modulator time window H 10 μs, M- number of multiplexer channels). The pulse response characteristic of the matched filter which performs compression of the signal is the complex-conjugate of the latter. When the modulator window is shorter than the signal duration, then the signal with a large base $W = \Delta F\Delta T$ is split into M equal fragments with a much shorter base $W = (\Delta F/M)(\Delta T/M) = W/M^2$ each and these are then completely compressed by means of dispersive delay lines and coherently added with corresponding time delays. The processor electronics are simplified by arranging the band filters and adjusting the distances between the diaphragms of the mask so as to ensure that, as the partly compressed signals run sequentially through all those diaphragms, partly compressed responses appear simultaneously at one instant of time $t = \Delta T$ only. The sequence of these signals must be a nonequidistant one and when it is encoded with "not more than one coincidence", then not more than one response will appear in the diaphragms at any other instant of time. The other processor components must be adjusted accordingly so as to ensure an interference-free output signal. The processor performance in both signal compression and panoramic survey modes is analyzed on the basis of simulation with a binary transparency, for a linear antenna array of consisting of nine elements. Figures 9; references 8.

UDC 621.396:535.8

Output Signal of Adaptive Acoustooptical Processor of Long Linear- Frequency-Modulation Signals

917K0062E Kiev IZVESTIYA VYSSHIKH UCHEBNYKH ZAVEDENIY: RADIOELEKTRONIKA in Russian Vol 33 No 8, Aug 90 pp 51-55

[Article by N. A. Yesepkina, A. P. Lavrov, and M. N. Ananyev

[Abstract] The performance of an adaptive acousto-optical processor of linear-frequency-modulation signals is evaluated by analyzing its output signal while it adapts to incoming signals with various rates of frequency change. The optical part of the processor includes a laser serving as light source followed by a beam widener, an acousto-optic modulator, an integrating lens, and a linear charge-coupled photodetector array in the focal plane of that lens operating in the time delay and storage mode. When the modulator is excited by an LFM signal much longer than the modulator time window, then a diffraction spot forms in the focal plane of the lens and moves across the photodetector surface in that plane at a constant velocity which depends on the rate of frequency modulation. An analysis of the luminance distribution over that spot reveals that both the spot width and of the maximum luminance at the point where it occurs depend on the phase lead. This dependence indicates the maximum range of phase lead angles $0 \leq \theta < \theta_{max}$ and thus also the maximum rate of frequency modulation the processor can handle, based on permissible changes in the processor output signal. Synchronous movement of the diffraction spot and the photosensors is considered first, the signal compression ratio in the processor being calculated for this case while taking into account that the spot is wider when the luminance is not uniformly distributed over the modulator aperture but tapers toward its edges. The effect of their being out of synchronism is evaluated next. The theoretical results are supplemented with and validated by experimental data, an acousto-optic modulator on a TeO_2 crystal with a center frequency $f_0 = 70$ MHz, a bandwidth $\Delta f = 20$ MHz, and a $T = 10$ μs wide time window having been tested on LFM signals of up to 80 ms duration with initial frequencies $f_i \geq 60$ MHz and final frequencies $f_e \leq 80$ MHz. A video pulse of 0.44 ms duration, corresponding to compression ratio of 180, was recorded with a 20 MHz wide LFM signal of 80 ms duration at the modulator input. Figures 3; references 5.

UDC 621.317.77

Statistical Characteristics of Output Signal From Acoustooptical Sum-Difference Phase Meter

917K0062F Kiev IZVESTIYA VYSSHIKH UCHEBNYKH ZAVEDENIY: RADIOELEKTRONIKA in Russian Vol 33 No 8, Aug 90 pp 70-73

[Article by A. Yu. Odintsov]

[Abstract] An acousto-optical instrument of the interference type for measuring the phase difference between signals of unknown frequency is proposed, interference of electric input signals being effected by sum- difference transformation and attendant conversion of phase modulation into amplitude modulation prior to acousto-optic conversion making it possible to replace one two-dimensional acousto-optic channel with four one-dimensional ones. The instrument includes a wideband 90° phase shifter which performs the Hilbert transformation, followed by two adders and two subtractors whose output signals enter each one of four identical acousto-optical spectrum analyzers with spatial integration. Their outputs are pairwise subtracted, whereupon the ratio of the two differences and the arc tangent of this ratio are computed. The latter gives an average estimate of the phase difference between spectral components. Each acousto-optical spectrum analyzer operates with a coherent light beam from a semiconductor laser, this beam being collimated by lens and then diffracted by a sound beam which comes from an acoustic light modulator with a transparent sound guide. Another lens transforms the diffracted light beam so that in its focal plane appears an amplitude-phase distribution of the light field, this distribution being described by the instantaneous spatial spectrum of that part of the electric signal which appears in the aperture of the acousto-optic interaction space and being read into a linear charge-coupled photosensor array. Identicality of all four acousto-optical spectrum analyzers is particularly easy to ensure, with the added advantage of size and power drain minimization, by building them with integrated-optics components. The output signal of each analyzer is formed by three products: signal at the one input by signal at same input, signal at one input by noise at same input, noise at one input by noise at same input. These components of each output signal are compensated, after pairwise subtraction in the respective quadratures. A performance analysis of this acousto-optical phase meter, supplemented with numerical calculations, indicates that its interference immunity is not worse than that of the optimum one. Figures 3; references 4.

UDC 621.391.266

Quasi-Optimum Algorithm of Correlational-Extremal Image Processing

917K0062G Kiev IZVESTIYA VYSSHIKH UCHEBNYKH ZAVEDENIY: RADIOELEKTRONIKA in Russian Vol 33 No 8, Aug 90 pp 83-84

[Article by D. A. Bezuglov]

[Abstract] A quasi-optimum algorithm of correlational-extremal image processing for radio navigation systems is constructed, an image appearing at any instant of time being in such a system compared to a standard one. Both images are defined in the L_2-space as functions of two coordinates x,y each, on corresponding segments of the plane. Both functions are formulated as double integrals

of discrete variables x,y. Into the L_2-space is then introduced a system of orthogonal functions and processing proceeds accordingly. The algorithm involving use of these functions is shown to shorten the necessary computations but to require a larger memory. The number of approximating polynomials, usually 4-12, is selected on the basis of required image representation accuracy. The approximation error is smallest with Karunen-Loew orthogonal polynomial basis and almost as small with ΣΠ expansion, although other basises such as Laguerre, Legendre, and Hermite polynomials or Walsh functions can be used. References 4.

UDC 621.391.193

Image Recognition in Presence of Color Background Interference

917K0062H Kiev IZVESTIYA VYSSHIKH UCHEBNYKH ZAVEDENIY: RADIOELEKTRONIKA in Russian Vol 33 No 8, Aug 90 pp 84-86

[Article by V. K. Baklitskiy]

[Abstract] Image recognition by correlational-extremal processing is analyzed for the effect of narrow-band background interference with an exponential correlation function, such an interference being called "color" interference and representing the most common form of clutter. Image recognition on the basis of the Bayes detection rule is considered, which requires calculation of the likelihood ratio equal to the ratio $W_{psj}(1)/W_{psj}(0)$ (a'posteriori probability densities of signal presence and signal absence respectively). When this ratio P satisfies the inequality $P < W_{prj}(0)/W_{prj}(1)$ (a'priori probability densities of signal absence and signal presence respectively), then the decision is presence of signal s_i. The algorithm of calculating the ratio P and testing that inequality takes into account the monotonicity of an exponential interference correlation function. Inasmuch as both sides of that inequality contain only positive quantities, it is expedient to take the logarithm of each. The algorithm can be executed most efficiently either by parallel and thus fast processing in a number of channels depending on the number of possible images, with a standard reference image in each channel, or by sequential and thus simpler but slower processing in a single channel with so many standard reference images successively inserted into it and the threshold correspondingly varied. Figures 1; references 2.

UDC 681.32:535

Optical Linear-Frequency-Modulation Correlator With Time Integration, Semiconductor Laser, and Charge-Coupled Photodetector

917K0062I Kiev IZVESTIYA VYSSHIKH UCHEBNYKH ZAVEDENIY: RADIOELEKTRONIKA in Russian Vol 33 No 8, Aug 90 pp 88-91

[Article by D. F. Gaynullin, N. N. Yevtikhiyev, and V. V. Perepelitsa]

[Abstract] An optical linear-frequency-modulation signal correlator for synthetic-aperture radar is described, one which operates with a semiconductor laser and a charge-coupled photodetector. The input signal to be identified modulates the laser radiation and the latter then passes through a collimator which, through a cylindrical focusing lens behind it, brightens the photosensitive region of the photodetector with a uniform intensity over the entire aperture. In front of the photodetector is placed a transparency-mask onto which a reference function T(x) has been recorded. The photodetector operates in the continuous scanning mode, with charge storage and time shift. The charge stored by its elements shifts in time from one cell to the next, the charge transfer time being called the time it takes for the charge shifting from the first cell to the last, whereupon it is displayed on the video monitor. The process is analyzed for a signal $S(t) = A\cos(\alpha t^2)$ $(-T/2 < t < T/2)$, α denoting the rate of frequency modulation and period T being equal to charge transfer time. For the purpose of optimizing such a correlator in terms of charge transfer time and frequency modulation, also the characteristic dimensions of black (opaque) and white (transparent) fringes on a binary mask, an experiment was performed with a GaAlAs-laser as light source (0.84 μm) delivering an average optical power of 3 mW. The photodetector was linear array of 512 charge-coupled devices, with autonomous control of its operation in the charge storage and time shift mode. Spatial integration was performed for two different masks. Both the signal-to-noise ratio and the resolution were found to become higher with an increase in the frequency deviation α. The constant component due to a large "crest" of the pedestal was eliminated by square-law detection, with some of the laser radiation diverted to an identical other detector and another mask, a negative of the T(x) mask placed in front of the latter. The output signal from this second photodetector had a constant component of the same magnitude as the output signal from the first one, but a peak shifted 180° from that in the output signal from the first one. Subtracting the two output signals canceled their constant components and doubled the amplitude, as long as the signal-to-noise ratio did not change. Figures 5; references 2.

UDC 681.7.068:621.396.61

Shaping Spatial Radiation Pattern of Transmitter Antenna Arrays With Fiber-Optic Signal Distribution System

917K0062J Kiev IZVESTIYA VYSSHIKH UCHEBNYKH ZAVEDENIY: RADIOELEKTRONIKA in Russian Vol 33 No 8, Aug 90 pp 95-97

[Article by A. N. Bratchikov, A. I. Kukshin, Ye. S. Puzakov, and Ye. V. Savin]

[Abstract] A radio-optical transmitter antenna array is synthesized, a a coherent-optics processor controlling both shape and position of its radiation pattern in space

and time and fiber-optic transmission lines, ideally distortionless ones, distributing the signals over an array of modules. Each module of the antenna array contains a radiator and a photodetector with a low-noise amplifier. These modules are connected to the space-time processor through a bundle of optical fibers, the entrance tips all lying in one plane P and forming an array topologically similar to the antenna array. The processor has two optical channels, one for the main beam and one for the reference beam. Both receive radiation from a common two- frequency source. The radiation pattern is both formed with the aid of a spatial real-time light modulator and then scanned in the main-beam channel which has received ω_1-frequency radiation. The reference beam is needed for photodetection in the heterodyne mode in its channel, which has received difference-frequency $\omega_2 = \omega_1 - \Omega$ radiation, so that the required amplitude-phase distribution can be then be transferred from the optical ω_1 onto the difference frequency Ω within the range up to millimetric waves. The radiation pattern is shaped by utilizing the property of a Fourier transformation that $E^*(\omega_x,\omega_y,1) = F(E^{-1}[E^*])$, where E^* denotes the complex amplitude-phase distribution of the optical field in the exit plane of the spatial real-time light modulator and F is the Fourier transformation operator. The amplitude-phase distribution of the optical field is perceived in the far zone and the Fourier transformation is performed in free space. The inverse Fourier transformation is performed by a lens directly in the plane P and from here transferred by the fiber bundle to the aperture of the antenna array, with a transformation ratio which ensures that the radiation pattern will have the required shape in the far zone. The operation of such a transmitter antenna arrays is demonstrated first in shaping a radiation pattern of arbitrary shape, including a multiple-beam one, and in single-lobe scanning with a narrow beam. In the first case the antenna radiation pattern is determined by the transmission function of the spatial real-time light modulator, while single-lobe scanning can be achieved with a much simpler time-independent transmission function on the transparency. Figures 2; references 2.

UDC 681.142.324

Using Computer for Determining Parameters of Periodic Components of Digital Signals

917K0055A Moscow METROLOGIYA in Russian No 7, Jul 90 pp 7-13

[Article by V. A. Dvinskikh]

[Abstract] An algorithm of fast Fourier transformation for analysis of a digital signal is constructed which includes sequential insertion of readings over several periods of the input process, rather than preliminary interpolation of the digital signal in the case of processes faster than the signal analysis, and thus makes it possible to perform the analysis in real time. An input process continuous in time and read out in the form of a digital signal is assumed to consist of a component periodic in time and other components plus interference. Harmonic analysis by this algorithm includes calculation of weight coefficients, only operations of addition or subtraction and multiplication being involved so that programming it on a K1800 high-speed LSI microprocessor becomes expedient in terms of computation time economy. The algorithm is extended to analysis of compound processes, superpositions of periodic processes whose frequencies are not multiples of one another. The algorithm is written in BASIC language. It has been tested for both accuracy and speed. References 9.

UDC 532.574.621.373.8.826

Potential Accuracy of Laser Doppler Velocimeters With Correlation of Photocounts

917K0055B Moscow METROLOGIYA in Russian No 7, Jul 90 pp 19-26

[Article by A. V. Averkin, A. I. Popov, and Ye. Ya. Stepanov]

[Abstract] The potential accuracy of a laser Doppler velocimeters is estimated, considering that it is determined by shot noise in the photodetector and that in such a velocimeter operating with correlation of photocounts this noise causes readings of the autocorrelation function to fluctuate. When multichannel digital correlators with clipping are used for measuring the autocorrelation function of signals in the form of photocount pulse sequences, then such an incoming sequence of M pulses is converted into a binary one according to the algorithm $M_{ij} = 1$ when $M \geq q$ and $M_{ij} = 0$ when $M < q$ (q- clipping level). Readings of the autocorrelation function are thus sums of photocounts recorded in given intervals of time equal to the pulse sampling period. Both the random error and the standard deviation of velocity estimates depend on the relation between the sampling period and the autocorrelation period, the latter being evaluated by the interpolation method with a parabolic spline so as to eliminate the error due to discreteness of the autocorrelation function readings. The effect of turbulence in the medium and the effect of a finite time-of-flight of light-scattering particles are first ignored, turbulence then taken into account and its intensity estimated on the basis of its readings in the case of Gaussian velocity fluctuations. An analysis of the established relations and the results of calculations based on them indicate that there are turbulence intensity levels at which the random errors of velocity estimates are minimum when based on the appropriate relation for the turbulence intensity. Using a Malvern 6200 laser Doppler velocimeter for measuring the turbulence intensity in gas streams has yielded a close agreement between its readings and theoretical estimates. Figures 1; references 1.

UDC 622.414

Phase Method of Acoustic Anemometry

917K0055C Moscow METROLOGIYA in Russian No 7, Jul 90 pp 39-43

[Article by S. Z. Shkundin and V. B. Lashin]

[Abstract] The phase method of measuring flow velocity and flow rate is theoretically analyzed, the purpose being to establish the missing phenomenological base and to reconcile the metrological characteristics of this method with a more precise theoretical model. The analysis is based on a one-dimensional wave equation which describes propagation of sound through a moving medium, both a source and detector of a plane wave being located in this medium at some given distance l apart. The phase shift of such a wave upon passage from the source to the detector is expressed in the form $\Delta = \omega Lc^{-2}v(1- M- M^2- ...)$ for a downstream traveling wave and $\Delta = \omega lc^{-2}v(1+ M+ M^2+ ...)$ for an upstream traveling wave. (ω- frequency of wave, v- velocity of stream, c- velocity of sound, $M = v/c$). For a specific application is considered propagation of sound through a gaseous medium inside an infinitely long rigid cylindrical waveguide-pipe. According to this model, the relation between the phase shift of a sound wave recorded by the anemometer and the velocity of stream is virtually a linear one within the low-velocity range. On this basis, anemometers operating by the phase method are now being developed at the Moscow Institute of Mining for use in mining. Figures 1; references 5.

UDC 621.38:001.018

Functional Electronic Element Design Principles

917K0024A Kiev ELEKTRONNOYE MODELIROVANIYE in Russian No 4, Jul-Aug 90 pp 50-54

[Article by A. B. Putilin, "Kvant" Scientific-Production Association, Moscow]

[Abstract] A previous work by the author demonstrated an approach to the description of physical systems based on analysis of physical processes and actual objects from the standpoint of a common classification. The use of structural-analytic vectors for functional electronic components is suggested, involving the composition of a structural-analytic matrix describing the functional electronic component, reflecting the composition of the structural-analytic vectors. This method allows various elements of the same physical nature to be compared. This approach is easily extended to analytic expressions describing particular cases as the equations of mathematical physics. The method generally allows a unified and qualitative information-based classification of functional electronic components, allowing the synthesis of elements based on their primary characteristics and determination of the location of each functional electronic component considering its characteristics. The method is applied to existing electronic components. Figures 8; References 4: Russian.

UDC 681.326.7

Design of a Convolution Module to Detect Postulated Class of Defects

917K0024B Kiev ELEKTRONNOYE MODELIROVANIYE in Russian No 4, Jul-Aug 90 pp 55-60

[Article by Ye. F. Berezkin, N. V. Yefremov, Moscow Engineering-Physics Institute]

[Abstract] A study is made of the problem of using a linear succession machine as a convolution module to detect all defects in a postulated class in an object of diagnosis. Two approaches to the construction of the convolution module are suggested suitable for detecting all defects of the given class and suitable for use as built-in testing devices for electronic equipment. Figures 3; References 7: Russian.

UDC 621.311.001.2

Improvement of Linear Mathematical-Economics Model to Optimize Structure of Electric Power System Generating Facilities

917K0024C Kiev ELEKTRONNOYE MODELIROVANIYE in Russian No 4, Jul-Aug 90 pp 80-85

[Article by A. V. Fomin, L. D. Khabachev, V. S. Sharygin, "Energosetproyekt" Institute, Leningrad]

[Abstract] Extended investigations have achieved a good level of detail in the machine implementation of a linear model to optimize the structure at the level of a unified power system. However, the increasing use of nuclear, pumped-storage, steam-gas and peak-demand power plants, consumer-demand regulators and other modern devices requires continued improvement of the model. Based on experimental calculations, this article establishes the required degree of detail of description of the operating mode in a linear mathematical-economic model to optimize the structure of generating facilities at the combined power system level. Methods are suggested for representing the new types of power installations recently put in use. A software system based on the use of standard and specialized programming facilities is suggested for linear mathematical-economic models to optimize power system structures. The use of the software system to solve scientific and design problems related to optimization of the structure of the generating facilities of the power system can double or triple the speed of solution of these problems. Figure 1, References 4: Russian

UDC 681.2:621.316.729

Use of Analog Relative-Frequency-Difference Converter in Phase Lock Systems

917K0022A Moscow IZMERITELNAYA TEKHNIKA in Russian No 7, Jul 90 pp 44-46

[Article by L. Kh. -G. Korsunskiy]

[Abstract] A phase-lock system for automatic frequency control with an auxiliary frequency locking loop in addition to the main phase locking loop is described, specifically one in which a discrete set of frequencies from below 1 Hz to 1 MHz can be synthesized for generating sine-wave voltages by linear and linear-step approximation. The main loop consists of a phase detector which receives signals from a fixed-divider dividing circuit, a summing and filter circuit built on an operational amplifier, a digital-to-analog converter, a tunable pulse generator, and a variable- divisor dividing circuit which feeds back into the phase detector. The auxiliary loop is formed by a frequency detector in parallel with the phase detector between the fixed-divisor dividing circuit and the summing and filter circuit. The summing device receives three input signals: 1) from the reference-voltage generator in the open preliminary frequency setting loop, 2) from the phase detector in the phase-lock automatic frequency control loop, 3) from the frequency detector in the automatic frequency control loop. The phase detector has a ramp characteristic and a structure analogous to that of a device which converts phase difference into a.c. voltage. The transfer function of the filter is the same for each of the three input signals. A performance analysis of the preliminary frequency setting device is followed by a stability analysis of the phase-lock automatic frequency control system "in the large" and then of the entire

frequency-phase automatic frequency control system. The results of this analysis indicate that using the frequency detector a device which converts relative difference of pulse repetition rates into d.c. voltage will both widen the locking band and shorten the locking time. Such a frequency detector is compatible with a phase detector which operates as both scanning converter of time integrals into d.c. voltages and sampler-storage, inasmuch as it compensates for the inadequate signal of such a phase detector in the case of a large frequency mismatch and the response speeds of both detectors are then of the same order of magnitude. Figures 2.

UDC 621.396.67.012.12

More Accurate Measurement of Antenna Characteristics on Basis of Apriori Information

917K0022B Moscow IZMERITELNAYA TEKHNIKA in Russian No 7, Jul 90 pp 46-48

[Article by R. I. Rumyantsev]

[Abstract] Measurement of antenna performance characteristics by the method of digital filtration and the characteristics of such filters are analyzed for ways to improve the accuracy of these measurements. Measurement of the field amplitude and phase distribution in the antenna aperture is considered specifically, assuming in the first approximation that the random field here is a uniform and ergodic one. Filtration through a spatial weight window is preferred to filtration through a frequency window, on account of the simpler algorithm. The algorithm involves smoothing the filter output (realization of the random field) by convolution of the latter and the window, followed by a Fourier transformation and estimation of the antenna radiation pattern. The algorithm is further simplified by determining the fitration parameters on the basis of mathematical simulation rather than by analytical determination of the relation between the statistical characteristics of the measurement error, the form of the actual field distribution, and the characteristics of the smoothing window. The radiation pattern of a rotating antenna was, for the purpose of an accuracy analysis and with the aid of a 1024-point fast Fourier transformation, reconstructed from two field distribution models with an M = 40-point linear aperture dimension each: a uniform one and a "cosine on pedestal" one. Random errors were filtered in four different ways with four different weight windows: 1) rectangular window, 2) cosine window, 3) Henning window, 4) Hamming window. The width of these windows was varied from 0.075M to M. As a result was obtained the dependence of both bias and dispersion of the radiation pattern estimate on the antenna rotation angle. An analysis of these results indicates that separate selection of window type and window width for the amplitude distribution and for the phase distribution is beneficial, considering that a optimum choice is different for each. The selection can be based on field distribution smoothing done for an antenna with known physical characteristics close to those of the tested one. Figures 1; references 3.

UDC 621.317.382.023

Temperature Field in Absorbing Wall of Coaxial Line

917K0022C Moscow IZMERITELNAYA TEKHNIKA in Russian No 7, Jul 90 pp 48-49

[Article by Yu. V. Shpagin and L. G. Martynenko]

[Abstract] A segment of a coaxial transmission line is considered where a rectangular window cut in the thick outer cylindrical conductor has been covered with a thin rectangular foil of a high-resistance alloy such as Constantan, to simulate a microwave wattmeter with an absorbing wall which does not constitute an inhomogeneity when inserted into a waveguide and whose presence thus does not distort the electromagnetic field inside. Heating of this "wall" by electromagnetic energy passing through such a coaxial line and the resulting temperature distribution over its surface are analyzed theoretically and on the basis of experimental data. Theoretical calculations are based on the basis of the equation of steady-state heat conduction, assuming not only that the wall is an infinitely long strip but also that the temperature at its boundaries with the outer conductor and its temperature profile across its thickness remain constant in time. The experimental data pertain to a 10 μm thick and 12 mm wide Constantan wall in a coaxial line with conductors 16 mm and 6.96 mm in diameter, measurements in an electromagnetic field of $\gamma = 3.2$ cm wavelength and a 10 W power having yielded temperature rises differing by not more than 10 percent from the theoretical 0.11°C. The error of power measurement is proportional to the error of temperature rise measurement, the proportionality factor depending on both initial and final temperatures. The ratio of highest to lowest wall temperatures measured along the coaxial line maximum is determined by only two parameters: $\eta = 2\pi d/\gamma$ and $U = (\alpha d^2/4\delta k)$ (α = heat transfer coefficient, d- width of wall = length of arc, δ- thickness of wall, k- thermal conductivity of wall material). Figures 1; references 8.

UDC 621.049.77.089.5:389.14:612.172.4

Metrological and Operating Characteristics of Microelectronic QRS- Detectors

917K0022D Moscow IZMERITELNAYA TEKHNIKA in Russian No 7, Jul 90 pp 50-51

[Article by B. I. Podlepetskiy and S. V. Torubarov]

[Abstract] Several types of QRS-detectors for converters of electrocardiogram signal into heartbeat rate are comparatively evaluated with respect to metrological and operating characteristics. An analog QRS-detector using

an operational amplifier is not only the structurally simplest one but also features high stability and reliability when under conditions of limited movements, while a QRS-detector with only digital signal processing ensures the necessary interference immunity and accuracy in a smaller size and at a lower cost than would an analog one. Such a QRS-detector has been built with a KM1813BYe1 signal processor made in the USSR and with a signal squarer but without differentiator. Squaring the signal eliminates dependence on the signal polarity and further raises the R-wave crest above the interference level. The time position of the R-wave crest is determined directly from the EKG signal so that a differentiator becomes unnecessary. As a third possibility is considered a hybrid QRS- detector, with analog filters but programmed digital detection. No one particular type of QRS-detector is the absolutely best one. The choice will depend on the specific biomedical application (human, animal), on the the condition of the object (healthy, under observation, ill), on the activity of the object (immobile, movable, freely moving), on the level of external electromagnetic interference, and also on the method of further data processing. For a moving healthy person, for example, a wireless data transmission channel is most desirable and miniaturization of the probe attached to the person becomes a very important criterion. In this case a higher interference immunity is achieved using an integrated-circuit radio transmitter which includes a simple analog QRS-detector, but a greater functional flexibility is achieved by using a transmitter of the EKG-signal and converting that signal into the heartbeat rate with the aid of a more intricate analog or digital QRS-detector in the receiver. The main obstacle to extensive use of digital data processing QRS-complexes is the limited availability of integrated microcircuits. Figures 1; references 4.

UDC 621.386.2

Television Image Generators in Radiation Fields

917K0015A TELEVIZIONNYYE DATCHIKI IZOBRAZHENIYA V RADIATSIONNYKH POLYAKH in Russian 1989 pp 4-8, 157

[Annotation, Preface and Table of Contents of book *Televizionnyye Datchiki Izobrazheniya v Radiatsionnykh Polyakh (Television Image Generators in Radiation Fields)* by V.M. Konyayev, S.S. Krasovskiy, I.N. Surikov and V.I. Flerov, Izdatelstvo "Zinatne," 1989, 157 pages]

[Text] Annotation

Television image generators are extensively employed in television optical systems in nuclear engineering, when using radioactive isotopes, and in nuclear and space research. The necessity of using these devices under conditions of exposure to radiation brings up a number of problems in their development and operation. When making the generators it is necessary to consider radiation effects in the major units and materials of structural elements, and to minimize their joint detrimental impact on operation of the devices as far as possible.

It is important for users of television image generators to have a means of reliably predicting their behavior under radiation conditions, and to know the levels of radiation at which the generators can be operated. This book examines radiation processes that occur in image generators, and their effect on operation of the devices. A comparison is made of the effectiveness of using various types of generators, which facilitates selection for service under exposure to radiation.

Tables 4, figures 86, references 230.

Preface

It has come to pass that two seemingly unrelated engineering fields, industrial television and nuclear power, have arisen and subsequently developed almost simultaneously. And from the very beginning they have been seen to be mutually dependent with a positive effect.

For nuclear engineering, television has been necessary as an effective means of remotely transmitting, recording and storing optical information from spaces with small geometric dimensions, or from space inaccessible to humans for a number of reasons, including considerations of radiation safety. By using a broad gamut of specialized television facilities produced both in the Soviet Union (series TSU, TES, STU) and elsewhere with a wide range of structural, functional and operational characteristics, some bottlenecks in the development of nuclear engineering and power have been overcome to a certain extent, or are being successfully overcome.

At the same time, the demands of the nuclear industry have stimulated the development of television, resulting in the advent of miniature television installations that are reliable and convenient to use, including under extreme conditions, their most important components being television image generators (TIGs).

A still greater interdependence shows up when one compares the history of development of television and engineering for space research. The famed advances in studies of outer space by unmanned probes have been achieved to no mean extent thanks to the high level of TIG parameters. At the same time, the demands of space engineering have been conducive to intensive development of industrial television, and have led to the advent of a considerable number of new TIGs.

A common feature of the use of television in these two fields so far apart—nuclear power and space engineering—is the presence of radiation fields that impact on all its components, including TIGs.

There is yet another field of engineering (the list could go on) where the use of TIGs is just as specific: various kinds of research and industrial isotope facilities where television is used for remote visual monitoring and control, especially the powerful isotope installations with ^{60}Co. Such facilities have widely penetrated into everyday life. The use of television in this case enables solution of many problems of remotely monitoring the movement of isotope rods, and makes it easy for service personnel to handle both routine tasks and problems that arise in emergencies.

The pattern of radiation fields that act on TIGs in these cases is quite erratic. In outer space one most frequently encounters weak radiation fluxes, but at the same time their action on TIGs is often of long duration. When used in nuclear power facilities and isotope installations, TIGs may be subjected to the action of high-intensity radiation fields. Let us note that although static radiation fields act on TIGs in most cases of application, it is sometimes important to know the response of the devices to pulsed radiation exposure as well. For example, such cases may occur in the case of solar flares in outer space. Pulsed radiation is also of interest in connection with the military use of TIGs.

The first publications on the impact of penetrating radiation on TIGs appeared on the very earliest stages of utilizing television in nuclear power and space engineering.

A considerable body of experimental data has now been accumulated on the influence of radiation either directly on TIGs, or on their individual components. However, due to the absence of systematized results (and those that are available are published in disparate divisions of the technical literature) and narrowly focused analysis, we have no clear concept at this time about the mechanism of the radiation impact on TIGs and the possibilities of utilizing them in radiation fields.

The authors of this book have set themselves the goal of using analysis of data in the literature and the results of

their own experimental research as a basis for ascertaining the mechanism of radiation action on TIGs, and then using these concepts as a basis for examining the problems that arise when making and using the devices under conditions of radiation exposure. The work should not be taken as a complete survey of publications on the investigated problem: this would exceed the limits of the tasks that the authors have set for themselves. And besides, such surveys have already been done on narrowly specialized issues relating to the problem.

Chapter 1 gives a brief description of the working principle and design approach of present-day TIGs, as well as characteristics of the radiation environment in which they are used.

Chapter 2 independently examines radiation effects in the entrance windows of TIGs. This is associated with the considerable impact that optical radiation effects in input windows have on the operation of all types of image generators, be they vacuum tubes or charge-coupled devices.

Radiation processes in vacuum TIGs are considered in Chapter 3. This group of TIGs includes multiplier phototubes, which are considered in some detail here because of their use in television systems with mechanical scanning, and also in view of the common nature of many radiation effects and the capability of using the large body of data available for multiplier phototubes.

Chapter 4 contains materials that characterize the radiation resistance of silicon-based solid state TIGs.

In presentation of materials, the authors have retained the terms and symbols used in Soviet publications.

V. M. Konyayev

Contents

PREFACE 5

Chapter 1: 1.1.

Chapter 1: Television Image Generators and the Radiation Environment in Which They Are Used 9

1.1. Basic information about image generators and their use in television systems 9

1.2. Radiation environment under actual conditions of use 15

Chapter 2: Radiation Effects in Input Window Materials 22

2.1. Induced optical absorption 22

2.2. Luminescence 43

2.3. Phosphorescence 51

2.4. Thermostimulated luminescence 58

2.5. Outgassing. Charge accumulation 66

Chapter 3: Vacuum Television Image Generators Under Conditions of Radiation Exposure 68

3.1. Multiplier phototubes and image dissector tubes. 68

3.2. Vidicons and supervidicons 78

Chapter 4: Solid State Television Image Generators Under Conditions of Radiation Exposure 82

4.1. Effects in silicon substrate 82

4.2. Effects in oxide of MOS structure 97

4.3. Functional photosensitive charge-coupled devices under conditions of radiation exposure 104

REFERENCES 144

UDC 621.313.32-81

New Generation of Turbogenerators With Air Cooling System

917K0029A Moscow ELEKTROTEKHNIKA in Russian No 9, Sep 90 pp 2-4

[Article by Ya. B. Danilevich, corresponding member, USSR Academy of Sciences, and G. S. Zhuravlev, candidate of technical sciences, All-Union Scientific Research Institute of Electrical Machines]

[Abstract] A new design of air-cooled two-pole turbogenerators similar to the KWU 160 MVA 3000 rpm machine (installed in Ambarli/Turkey) and the ABB 188 MVA 3000 rpm machine (CIGRE) is proposed, an open air cycle being preferred because it eliminates the need for air condensers in the ducts and thus simplifies the stator structure. Tangential air flow is recommended for cooling the stator from the gap, air blast being preferred to air exhaust for better cooling of the coil heads. Excessive heating of the two end stacks of the iron core can be avoided by making them shorter than the inner stacks and beveling them. Special heaters should keep the air inside the machine warm during shutdowns, which will prevent vapor condensation on the winding insulation. A rotor construction with radial ducts and with axial ducts under the slots is recommended for direct air cooling of the entire rotor barrel, with the pressure head developed by centrifugal forces during rotation boosting the pressure head developed by the fan. The shaft can be made shorter by resorting to shielded bearings and an overhang brushless exciter will be smaller than one of the thyristor version, considering that size and weight reduction being also important design criteria. All these features have been incorporated in the design of a 25 MVA - 6.3 kV - 3000 rpm turbogenerator, its efficiency being 97.6 percent at a 0.80 power factor (short-circuit ratio 0.636, transient reactance 16.1 percent) and its specific weight being 1.40 kg/kVA. Figures 3; tables 1; references 10.

UDC 621.316.542.064.42

Self-Generating Arc Quenchers in SF_6 Circuit Breakers

917K0029B Moscow ELEKTROTEKHNIKA in Russian No 9, Sep 90 pp 4-9

[L. N. Matkovskaya, engineer, Scientific Research Institute of Scientific-Industrial Association 'Uralelektrotyazhmash' (Ural Heavy Electrical Machinery)]

[Abstract] A survey of self-regenerative arc quenchers for 80+ kV and SF_6 circuit breakers is given which covers not only the state of the art worldwide but also the recent history of and current trends in their development. In the basic such device a pressure rise is generated by the arc itself inside an enclosure and the latter is then opened for admission of the blast. Such an arc quenchers can be combined with magnetic one using an electromagnet or permanent magnets, the arc being first elongated by the magnetic field and then quenched. It can also be combined with a plunger- driven arc quencher which operates either before or together with the basic one. The survey includes the general design and specific applications. It also includes a historical outline of inventive and publishing activity over the 1969-88 period. Figures 5.

UDC 621.313.12.025.047:661.66.2.002.3

Carbon Slip Rings For A.C. Generators

917K0029C Moscow ELEKTROTEKHNIKA in Russian No 9, Sep 90 pp 42-45

[Article by A. S. Fialkov, doctor of technical sciences, Ye. F. Kolpikova, candidate of chemical sciences, B. A. Gluskin, candidate of technical sciences, Yu. S. Krylov, candidate of technical sciences, and V. M. Kormilitsyn, engineer]

[Abstract] An experimental study was made concerning replacement of copper with a composite carbon material as both electrical conductor and antifriction material for slip rings in automobile alternators, three grades of a composite based on graphite and a high-molecular polymer having been selected for this application. Slip rings 10.5 mm long with 32/25 mm outside and inside diameters were molded on a hydraulic press under a pressure of 1500 kgf/cm^2, after 8 mm thick plates 12.5x25 mm^2 in cross-section were tested for electrophysical and mechanical characteristics. The best of these materials has an electrical resistivity of 19.0 ohm.mm, a compressive strength of 34.1 MPa, a flexural strength of 51.2 MPa, and a hardness of 178)x10^4 range. The density of the slip rings was 2.0 g/cm^3, much higher than that of the 6 mm thick and 6.5 mm wide EG electrographitic brushes with which they were tested. Their overall open porosity did not exceed 0.5 percent. Microstructural examination was done under a JSMCF-35 "Jeol" scanning electron microscope. Thermal tests were performed with an MOM derivatograph in air, the temperature rising 10°C/min in each test. Their oxidation resistance was found to deteriorate sharply as the temperature rose above 350°C. Slip rings of that material were selected for wear tests, grade EG2A brushes having been selected in preference to EG51, EG61, EG75 brushes on account of their lowest friction and electrical contact resistance. In a 4000 h test corresponding to 100,000 km automobile "mileage" the (+) brush and and its slip ring wore down 0.44 mm and 0.41 mm respectively while the (-) brush and its slip ring wore down 0.63 mm and 0.19 mm respectively, under a voltage drop of 0.0.05-0.07 V on each side. Subsequent tests at the Scientific Research Institute "Avtoelektronika" (Automotive Electronics) yielded a 0.03 mm wear of the (+) brush and a 0.015 mm wear of the (-) brush after 400 h at an ambient temperature of 95-100°C, with the alternator running at a speed of 8000 rpm (100,000 km automobile "mileage") under an electric load of 32-34 A. Figures 4; tables 2; references 6.

UDC [621.865:681.325].001.4

Optimization of K1801VM2-Based Microprocessor Control for Electric Positioning Drive

917K0029D Moscow ELEKTROTEKHNIKA in Russian No 9, Sep 90 pp 45-49

[Article by V. S. Yudenkov, candidate of technical sciences, Yu. V. Lopatin, engineer, and I. M. Gaynutdinov, Belorussian Polytechnic Institute]

[Abstract] Automatic control of the electric positioning drive which moves the horizontal platform carrying an instrument to be tested in a gyroscope suspension system is considered, this platform having three degrees of freedom with a d.c. electric drive for each. Their speeds and positioning movements are controlled by a microprocessor acting on the armature current in accordance with given laws. Such an automatic control system includes accordingly a PID (proportional-integral-differential) speed regulator with a relay element and a position regulator. Each drive is program controlled in the pulse-width mode by digital codes from the microprocessor, integration and differentiation being replaced with summation and with calculation of finite difference respectively. The dynamics and the performance of such a system are analyzed for accuracy and stability of the acceleration-run-deceleration cycle, whereupon they are optimized for minimum integral-square speed error and minimum energy loss. The control algorithm has been written in ASSEMBLER language in the K1801VM2 command system, the programs for the regulators to be stored in the lower-level read-only memory which the upper-level timer triggers every 1 ms. Figures 3; references 4.

UDC 621.3.002.6:616.082

Experience and Problems in Producing Newest Medical Equipment for Mass Use

917K0029E Moscow ELEKTROTEKHNIKA in Russian No 9, Sep 90 pp 52-55

[Article by V. I. Adasko, doctor of technical sciences, A. B. Galitskiy, engineer, Yu. V. Chirkov, candidate of biological sciences, V. P. Chekhonin, engineer, V. F. Lavrentyev, engineer, and V. I. Glukhov, engineer]

[Abstract] Specialists at the All-Union Scientific Research Institute of Electromechanics, Istra branch, are now developing programmable medicine dispensers with appropriate sugar or blood counters for personal and laboratory use as well as electrical stimulators of human organs. Two insulin dispensers, DLV-1 and NDL-3 costing 1750 rubles and 740 rubles respectively, are already produced commercially by the Sarana Industrial Association "Vypryamitel" (Rectifier). Use of these devices makes consumption of medicine much more economical and greatly reduces the work load of medical personnel. Excellent dispensers now produced are the second- generation DLV-2 and the DG-1 hypodermic dispenser (developed jointly with the All-Union Cardiological Science Center) which uses an electric field for transporting molecules of the substance from a porous storage disk. Further development of third-generation dispensers should will most likely be a multichannel configuration for simultaneous dispensation of six-10 different substances and built-in special-purpose microprocessors. Electrical stimulators now being developed are the TsMG-1 cystomanograph with a mechanotron transducer for examination of the bladder and its sphincter system, the ESM-1P/1N electrical stimulators of the bladder sphincter, and the ESD-2P/2N-NCh electrical breathing stimulators. Further development of stimulators as well as of dispensers must aim at moderation of their cost and maximum reliability, simple construction and easy handling, quick readiness for use, fast and reliable accurate readout, and life. This will require availability of custom-made special electronic components and inexpensive reprogrammable low-power microprocessors, also special materials, microconductors, and microelectrodes for modular construction. Figures 4.

UDC 621.31

New Engineering Decisions for Primary Coal Crushing Equipment at Thermal Power Plants

917K0038A Kiev ENERGETIKA I ELEKTRIFIKATSIYA in Russian No 3, Jul-Sep 90 pp 4-7

[Article by G. P. Berlyavskiy, B. I. Pasko, L. A. Boyko, Southern Heat Engineering Institute]

[Abstract] Problems with the primary crushing and grinding equipment used at coal-fired power plants are considered. A new installation for primary crushing of frozen and monolithic solid fuel avoids many of these problems. The drive for the transportation of the milling cutter is stationary and installed outside the hopper. The cutter moves on horizontal rails riding on sliders with two vertical strips imitating wheel rims. The milling cutter is moved by a chain which forms a continuous loop around drive sprockets at each end of the track. The center of the gravity of the milling cutter is lower than in previous models. The force on the drive has been increased by decreasing the speed of movement of the cutter. Two electric motors operate through four-stage reducing gears. A special cutting element has been designed with hard-alloy lining. 16 such installations are now in operation at seven coal-fired plants. Figures 5; References 5: Russian.

UDC 621.31

Repair of Low-Voltage Winding Insulation of Power Transformers With Compound Insulators

917K0038B Kiev ENERGETIKA I ELEKTRIFIKATSIYA in Russian No 3, Jul-Sep 90 pp 31-32

[Article by V. I. Kostin, Kirov Mobile Power Plant]

[Abstract] A method is suggested for repairing the insulation of the insulators used with the low-voltage windings of transformers at the point of installation of the transformer. 1) Disconnect cable from insulator. 2) Measure resistance of insulation. 3) Place two locknuts on insulator 10 mm from sealing nut. 4) Use locknuts to prevent rotation of rod. 5) Back off sealing nut by 10 mm and raise sealing washers, holding down porcelain insulator. 6) Press rod downward 2-4 mm without rotation, allowing 150-200 g transformer oil to rise and leak outward. 7) Raise rod back up, return sealing washer to position and retighten sealing nut. Figure 1.

UDC 621.315.62

Progressive Technology For Manufacture of High-Voltage Insulators

917K0038C Kiev ENERGETIKA I ELEKTRIFIKATSIYA in Russian No 3, Jul-Sep 90 pp 32-34

[Article by B. I. Daydash, V. A. Aleko, K. N. Logvinov, I. M. Sova, Slavyansk Affiliate, All-Union Scientific Research Institute of Electroceramics; "Elektrofarfor" Scientific-Production Association]

[Abstract] A new and progressive process is described for forming porcelain insulators with spiral ribs by drawing them directly from a vacuum press. Rotation of the stage used in the drawing process is monitored by the interruption of a light beam by a propellor-shaped disk mounted on the stage, allowing the rotation rate to be carefully controlled. A diagram of the installation and photograph of the insulators produced are presented. This waste-free process of continuous formation of insulators with spiral ribs can be used to create industrial installations and automated production lines to produce a number of high-voltage insulators while significantly reducing the length of the production process and greatly decreasing the expenditure of materials and labor. Figures 3; References 7: Russian.

UDC 621.31

Automated PC-Based Workstation For Diagnosis of Oil-Filled Power Equipment

917K0038D Kiev ENERGETIKA I ELEKTRIFIKATSIYA in Russian No 3, Jul-Sep 90 pp 37-40

[Article by V. B. Vidzigovskiy, V. A. Kacharov, A. N. Nesterenko, V. B. Polishchuk, Yu. N. Potapenko, "Kievenergo" Planning-Finance Department, "Energoinformatika" Fire-Safety Department, Inter-Industry Scientific Center for Programming Technology]

[Abstract] An automated workstation has been developed by the authors' organizations for diagnosis of oil-filled electric power equipment. The workstation is based on a personal computer and utilizes artificial intelligence methods. The workstation consists of three parts: a data base management system, the software, including supplementary programs for processing chromatographic information and programs to recognize the status of the equipment according to "rigid" algorithms, and a diagnostic decision support system. A classification expert system is used, with menus in three windows. The expert system can provide consultation to help the user evaluate the results of analysis, to provide recommendations concerning further use of equipment, sampling intervals for analysis and the need for various electrical tests. The software is written for IBM PC/XT/AT compatible computers. References 2: Russian.

UDC 621.31.71

Fundamental Concepts for the Future Development of Electric Power Engineering

917K0027A Moscow ELEKTRICHESKIYE STANTSII in Russian No 8, Aug 90 pp 2-9

[Article by L. S. Popyrin]

[Abstract] A proposed policy outlining the future development of electric power engineering in light of the new economic conditions is given. Several objective factors responsible for inefficiencies, irregularities and poor performance in the field of electric power production are discussed, including obsolescence and wear of physical plant equipment, inefficient structural design of power production capabilities, a shortage of back-up systems and poor efficiency of heat supply systems. Future development is tied to increased electrification of industry and energy used per worker. The current and future breakdown of electricity consumption by economic field through the year 2010 is given. Strategies for efficient energy savings are outlined. Several measures are proposed for more efficient utilization of such natural resources as gas, oil and fuel, including more thorough refinement of petroleum products; increased levels of coal extraction; manual labor savings and more certain modifications of natural gas production. Present and future power output of nuclear, condensation, thermoelectric and gas- and coal-fired power plants in the USSR are listed by region. The role of nontraditional energy sources in future power production is discussed together with environmental protection measures in the field of power engineering.

Three-Tiered Management Structure For Power Engineering Under Conditions of Complete Cost-Accounting and Self-Financing

917K0027B Moscow ELEKTRICHESKIYE STANTSII in Russian No 8, Aug 90 pp 13-20

[Article by E. F. Makarov]

[Abstract] The proposed changes to implement a three-tiered management structure for power engineering at the Moscow Regional Directorate of the Power Production Industry, Ministry of Power Engineering and Electrification, are outlined and a block diagram of the design is provided. Under this plan the Moscow Regional Directorate will have five power distribution zones (Moscow, Northern, Southern, Eastern and Western). The changes that must be introduced in the 0.4 to 35 kV, 0.4-220 kV and 110 kV power distribution networks to support the consolidation this new plan will require are outlined. Personnel changes in management, supervision and control and repair facilities are specified along with the new responsibilities of regional and local managers. Diagrams outlining such changes are provided together with a list of additional measures to be taken to improve management and reduce costs of production.

UDC 621.315.1.027.875

Modern 750 kV Power Transmission Lines

917K0027C Moscow ELEKTRICHESKIYE STANTSII in Russian No 8, Aug 90 pp 63-68

[Article by A.N. Sherentsis]

[Abstract] The development of a modern distributed 750 kV power transmission line network in the USSR for power distribution between power pools and for delivering power from atomic and thermal power plants is discussed. Such design factors as power load capacity; automatic reconnection and disconnection; lightening protection; support mast design; line insulation and distance between phases are examined. It is determined from this analysis that automatic reclosing is one of the primary factors for improving the reliability of 750 kV power transmission lines, while approximately thirty percent of all 750 kV power line failures are found to be caused by improper operation of safety equipment and operator errors. A variety of insulator string designs (the PSK 210-A and PSK 210-B; the PS30-A and both the PS-12-A and PS-22-A designs) are also compared for both 750 and 500 kV power transmission lines. The applications of such designs in both rural and urban areas are considered.

UDC 621.313.332

Problems of Autonomous Electric Power Generation and Possible Solutions

917K0056A Kiev TEKHNICHESKAYA ELEKTRODINAMIKA in Russian
No 5, Sep-Oct 90 pp 70-77

[Article by A. I. Lishchenko, doctor of technical sciences, Institute of Electrodynamics, UkSSR Academy of Sciences, Kiev]

[Abstract] Modern autonomous electric power generation covers power ratings from 1 kW to 100 MW at voltage levels from 12 V to 10 kV d.c. and up to 5000 Hz a.c. The principal problem before the engineering community is optimization of the electromechanical energy conversion process. The problem is rather complex, but can be broken down into four closely interrelated ones: 1) minimizing size and weight of electrical machines with attendant conservation of active materials, 2) minimizing basic and additional power losses for maximum possible efficiency, 3) optimizing the quality of generated electric energy and the generator performance during transients as well as under normal conditions, 4) ensuring high reliability of generators during normal operation as well as during transients and faults, also ensuring their viability under extremely severe operating conditions. The theoretical basis for solving this complex of problems rests essentially on three laws: 1) Faraday's induced e.m.f. $e = - d\Phi/dt = B_0lv$, 2) Ampere's current in a circuit $I = \Sigma H_il_i$, 3) Ampere's force of magnetic field on current-carrying conductor $F = B_0lI$ (Φ- magnetic flux, B_0- magnetic induction, H- magnetic field intensity, l- length of conductor or conductor segment, v- velocity of conductor). Application of these laws in appropriate form and, if necessary, modified to rotating electric machines leads to the obvious choice of high-speed machines, but the advantages they offer must be weighed against the serious mechanical requirements and constraints. The rotor thus becomes the key component and, to illustrate this, various rotors in the intermediate size range of 1.5 m in diameter are considered: laminated wound rotors, solid rotors with polyphase winding for induction generators and cylindrical synchronous, solid rotors with squirrel cage, slotted solid rotors without winding for induction generators and homopolar inductor generators, and smooth rotors without winding for induction generators only. Induction generators require a special source of reactive power for autonomous operation without access to a power network or a synchronous generator. Synchronous generators require a field excitation system, which needs to be optimized along with the machine it serves. The two basic types of excitation systems are capacitive and solid-state ones. A new type of induction motor is one with an excitation system which consists of a storage battery and thyristor-inverter bank. Replacement of the latter with a transistor-inverter bank eliminates forced commutation, which results not only in appreciable size reduction and higher interference immunity but also broader controllability. Contributions made by the Institute of Electrodynamics to optimization of autonomous electric power generation is reflected in extensive mathematical modeling activity, design calculations, and hardware development. References 12.

Low-Power High-Voltage Sources

917K0056B Kiev TEKHNICHESKAYA ELEKTRODINAMIKA in Russian
No 5, Sep-Oct 90 p 110

[Article by A. A. Penin, Special Design and Manufacturing Engineering Office for Solid-State Electronics, Kishinev]

[Abstract] Three low-power high-voltage sources for laboratory practice, electrostatic coating, ionization chambers, electron and ion devices, and photomultiplier power supply are described. They are the IVN-3 (output voltage 100-3000 V, maximum load current 3.5 mA, operating in either voltage or current stabilization mode with visual mode indication, manual or digitally programmed high-voltage setting, maximum amplitude of voltage fluctuations 5 mV, maximum long-time voltage instability 0.01 percent), the IVN-80 (output voltage 3-80 kV, maximum load current 100 μA, analog output voltage measurement and analog external remote control of output voltage, maximum amplitude of voltage fluctuations 100 V, maximum voltage instability 1 percent, power requirement 30 W), and the IVN-70 (output voltage 70 kV, operating in current stabilization mode within 3-60 μA current stabilization range, maximum power requirement 60 W). All three are shielded against spark discharge in the load circuit, the IVN-3 with automatic voltage recovery. While the overall dimensions of both the IVN-70 and the IVN-80 are 250x250x110 mm^3, the IVN-3 has the same dimensions as the CAMAC standard module 2M.

Automatic Control and Monitoring Device AVTOSHCHIT for Nonconventional Electric Energy Sources

917K0056C Kiev TEKHNICHESKAYA ELEKTRODINAMIKA in Russian
No 5, Sep-Oct 90, p 111

[Article by Ye. V. Shevchenko, Institute of Electrodynamics, UkSSR Academy of Sciences]

[Abstract] An automatic control and monitoring device for autonomous plants running on wind electric or solar electric power with storage batteries as alternate energy source is described, this AVTOSHCHIT device being also usable in facilities such as telephone exchanges or radio relay stations where storage batteries are used as standby power supply. It responds to information about the state of such a plant and accordingly switches it either on or off. In the case of an impending failure, it disconnects the user from the plant and lights up a lamp to indicate the need for fault locating. It is rated for up to

6 kW power plants using 220/380 V a.c. wind electric generator sets and for 110 or 220 V d.c. storage batteries with correspondingly 160 or 80 A.h capacity. It automatically connects the battery to a charger during wind activity and disconnects it when charging has been completed, at that time also switches the wind electric generator set into the heat supply mode. It automatically connects the battery back to the charger when boosting is required during fluctuating wind activity. Through a distance relay, it disconnects the generator set as wind activity ceases and reconnects it as wind activity picks up. It also responds to information about the heat supply system and disconnects the latter from the generator set in up to 10 emergency situations including excessive drop of hot water level, excessive rise of hot water temperature, loss of water circulation, and excessively high room temperature. There is no commercially produced device like this available yet.

UDC 535.2:621.372.8:535.01

Calculation of Calibration Characteristics of Optical Analyzers for Fiber Diameter Measurement Taking Into Account Spectral Characteristics of Radiation Source and of Photodetector

917K0030A Minsk ZHURNAL PRIKLADNOY SPEKTROSKOPII in Russian Vol 53 No 3, Sep 90 pp 470-475

[Article by V. I. Ovod, Kiev Polytechnic Institute]

[Abstract] The calibration characteristics of optical analyzers for fiber diameter measurement are calculated, following an analysis of such measurements with the spectral characteristics of both radiation source and photodetector taken into account. First is considered a monochromatic laser beam scanning a fiber. The analyzer response signal is in this case proportional to the product of five parameters: power of laser beam P (in watts), absolute spectral sensitivity of photodetector to light of maximum- sensitivity wavelength $S_{\gamma\ max}$ (A/watt), relative photodetector sensitivity to light of given wavelength S_γ, relative scattering cross-section of illuminated fiber segment $\sigma_{1\gamma}$ divided by area of illuminated fiber segment, and spectral transmission coefficient of analyzer optics for light of given wavelength τ_γ. The proportionality factor is the product of two coefficients, one characterizing the nonuniformity of fiber illumination, independent of the wavelength, and one characterizing the optical-to-electric signal conversion by the analyzer electronics. Calibrating calculations are best made for a rectangular photodetector aperture, inasmuch as waves scattered by a fiber are cylindrical, with its center in the plane of scanning by a laser beam crossing the fiber perpendicularly to its axis. Next is considered a polychromatic scanning radiation beam and the parameters are modified accordingly to account for the transformation of the calibration characteristics. Measurements were made on an iron fiber and on a quartz- glass fiber, first with a laser beam and then with a polychromatic radiation beam. The results indicate that the calibration characteristics of an analyzer do not depend on the optical properties of fibers made of strongly absorbing materials. They also indicate that using a polychromatic radiation source is preferable, inasmuch as it is easier than with a laser beam to ensure high accuracy by selecting the wavelength at which the mean value of diameter readings will fall within the range of highest sensitivity. Figures 3; references 14.

UDC 535.34:621.315.592

Infrared Radiation Absorption By Ge-Doped Silicon After Neutron Bombardment

917K0030B Minsk ZHURNAL PRIKLADNOY SPEKTROSKOPII in Russian Vol 53 No 3, pp 499-502

[Article by V. V. Borshchenskiy, D. I. Brinkevich, and V. V. Petrov, Belorussian State University imeni V. I. Lenin, Minsk]

[Abstract] An experimental study silicon was made concerning the effect of Ge impurity on the spectrum of infrared radiation absorption after neutron bombardment. Crystals of p-Si with an initial electrical resistivity of 20 ohm.cm were doped with Ge to $3x10^{18}$-$1.9x10^{19}$ cm^{-3} concentrations during their growth from a melt by the Czochralski process. The concentrations of interstitial oxygen and nodal carbon, according to the respective 9.1 μm and 16.5 μm absorption bands, were then found to be $9.0x10^{17}$ cm^{-3} and $5.8x10^{16}$ cm^{-3} respectively. Control specimens of identical p-Si crystals without Ge impurity were tested alongside the doped ones. All were bombarded with neutron fluences of $1x10^{15}$-$1x10^{17}$ cm^{-2}, the ratio of thermal neutrons to fast neutrons being approximately 10:1. They were then isochronously annealed at temperatures ranging from 100°C to 500°C in 25°C increments, for 15 minutes at each. The infrared absorption spectra were recorded at 80 K and 300 K temperatures in Specord 75IR and Specord 61IR spectrophotometers. After bombardment were recorded the 830 cm^{-1} A-center band, the 5500 cm^{-1} W-bivacancy band, the 488 cm^{-1} deformation peak, and nonselective near-edge absorption within the 2-4 μm range. Annealing gave rise to new absorption bands: 890 cm^{-1} V-O_2 band, 864 cm^{-1} band of an unidentified center, weak 829,842,848 cm^{-1} bands of radiative-thermal A-center companion centers containing oxygen, and about 20 selective "high-order" bands within the 4.5-14.5 μm range. No centers containing Ge atoms were revealed, this isovalent impurity not having significantly influenced formation and annealing of V-O_2 centers (890 cm^{-1} band) and of the unidentified centers (864 cm^{-1} band) but having influenced annealing of A-centers. The mechanism of this influence could be either dissociation of such a defect into its components and migration as a whole toward a sink or capture by it of an interstitial O or Si atom. Oxygen was found to drain A-centers more effectively in p-Si:Ge crystals than in the pure p-Si control crystals, most likely owing to the lower concentration of interstitial defects in p-Si:Ge. Figures 2; references 8.

UDC 681.785.55:543.42

Trends in the Specifications of Series-Manufactured Nonscanning Ultraviolet Spectrophotometers

917K0026A Leningrad OPTIKO-MEKHANICHESKAYA PROMYSHLENNOST in Russian No 8, Aug 90 pp 3-13

[Article by B. I. Liflyandchik, A. V. Maliy]

[Abstract] The principal designs of mass-manufactured nonscanning ultraviolet spectrophotometers available worldwide are analyzed and compared. Only spectrophotometers with slit monochromators are considered. Such performance factors as photometric error; wavelength scale errors; spectral width of the monochromator slit; interference range; photometric range and operational spectral range are compared for the CE 2202 (Cecil); UV-120-02 (Shimadzu);

SF-46 (Soviet); Novaspec (LKB); Lambda 1A (Perkin-Elmer); SPS (Vital); PU 8620 (Phillips); DU-62 (Beckman); 258 (Ciba-Corning) and U-1100 (Hitachi) designs. The types of data display devices used with these instruments are outlined and prospects for the development of nonscanning spectrophotometers are considered.

UDC 621.391.8

Nonhomothetic Transformation of a Background Interference Domain in Multispectrum Systems With Different Fields

917K0026B Leningrad
OPTIKO-MEKHANICHESKAYA
PROMYSHLENNOST in Russian
No 8, Aug 90 pp 14-16

[Article by Yu. P. Safronov]

[Abstract] The nonhomothetic transformation of a background interference domain in a space of primary factors is derived for multispectrum systems with different fields with a variable fill factor. The primary factor for such systems is the effective average luminance for the instantaneous field of view; the set of primary factors for all channels in a multispecrum system forms an N-dimensional space of primary factors. These factors are used to determine the coordinates of a random point in the multidimensional space and to assign this point to either the background interference domain or the legitimate signal domain. A diagram of the nonhomothetic transformation is given.

UDC 535.31

Investigation of Wavefront Restoration Accuracy by Interferogram Processing

917K0026C Leningrad
OPTIKO-MEKHANICHESKAYA
PROMYSHLENNOST in Russian
No 8, Aug 90 pp 17-20

[Article by M.A. Gan, S.I. Ustinov, V.V. Kotov, I.V. Ivanova]

[Abstract] The restoration of signal wavefronts by processing a single interferogram and several interferograms is analyzed together with the resulting errors of these processes. The wavefront in the global interpolation in this analysis is represented as two-dimensional power polynomials. The coefficients of the polynomials are found by the least squares method. An expression is then derived that makes it possible to calculate the two-dimensional topography of the wavefront restoration accuracy at the system pupil. Two different wavefront restoration techniques are compared and a test calculation of wavefront deformation is carried out.

UDC 535.41:778.38

Recording of Lateral Shear Holographic Interferograms By Spatial Filtering

917K0026D Leningrad
OPTIKO-MEKHANICHESKAYA
PROMYSHLENNOST in Russian
No 8, Aug 90 pp 20-24

[Article by V. G. Gusev]

[Abstract] Holographic recording of the imaginary image of a frosted screen is used to substantiate the claim that illumination of a test lens or objective by diffusely scattered coherent radiation can be used to form lateral shear interferograms that characterize the wave abberations of the test object. An expression is derived for describing the speckle-structure produced by the experimental set-up constructed to test this conjecture. This optical configuration consists of the frosted screen, a photographic plate, a reference beam, an aperture diagram and a screen with a small aperture as well as several lenses. The resulting speckle-structure is modulated by the interference bands; the interference pattern takes the form of lateral shear interferograms in bands of infinite width and is generated by axial wave abberations localized in the plane of the system pupil. It is determined that in order to record this diffraction pattern at the (minus) first order, spatial filtering must be carried out in the image plane of the lens pupil and a Fourier transform must be applied to the diffracted field.

UDC 681.787.062.2

Determination of Spherical Surface Errors By Spherical Beam Interferometry

917K0026E Leningrad
OPTIKO-MEKHANICHESKAYA
PROMYSHLENNOST in Russian
No 8, Aug 90 pp 32-35

[Article by V. B. Gubin, V. N. Sharonov]

[Abstract] A mathematical processing technique is proposed for analysis of interferograms that uses an analytical approximation of spherical surfaces. The technique employs polynomials defined in the plane of a basis sphere of unitary radius. A set of basis functions is also derived for describing the position and shape of surface areas similar to the basis surface with centers near the center of the basis sphere. A variety of interferogram schemes are investigated. It is determined that a single interferogram is both necessary and sufficient for determining the sum errors of a pair of spherical surfaces.

END OF FICHE

DATE FILMED

12 Feb. 1991